

第五章

表面等离激元光学和量子体系的交叉研究

结合了光子学和电子学的优点，通过将光场压缩在纳米尺度，允许在纳米尺度上研究光与物质相互作用。

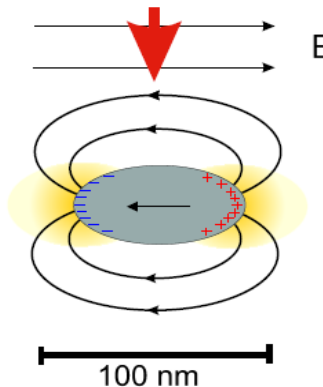
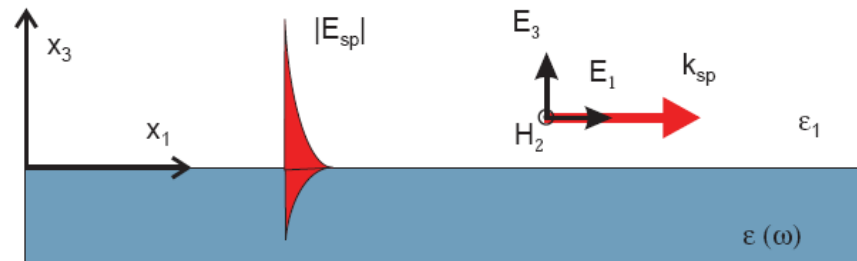
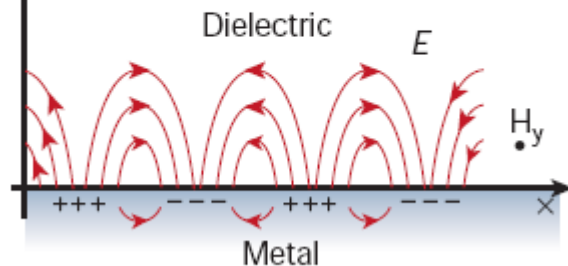
表面等离激元本质上是电磁波，具有波粒二象性。

在未来的计算机中光子能够代替电子吗？光子回路体积小，易于集成，损耗小，传的快，但是光子间没有相互作用，实现量子操控比较困难。光子与表面等离激元间的交换弥补了这一不足，可在单光子探测，纠缠，可控相位门，量子的非线性效应方面有应用。

Surface plasmon polariton (SPP)

a

SPP: collective oscillations of free electrons evanescent EM mode bound to surface



Localized SP or SPR:
localized oscillation
strong local field

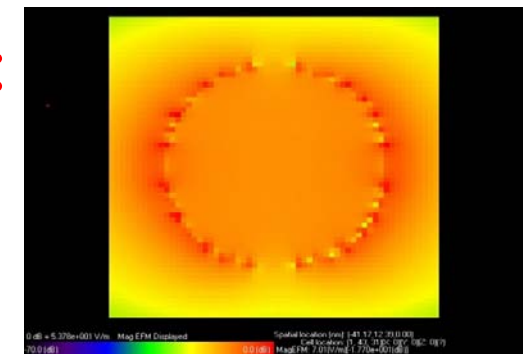


Figure 1.3: Particle plasmon



ultrasmall optical mode volume V_m

William L. Barnes, Alain Dereux & Thomas W. Ebbesen, nature, 424, 824 (2003);
V. Zayatsa, et al, Phys Rep. 2005, 408:131–314;

What's new for quantum emitters with ultrasmall optical mode V_m ?

Weak coupling: Purcell factor $F = \gamma / \gamma_0$
anisotropic electric mode density of oscillations
→ anisotropic optical mode density →
anisotropic decay rates → enhanced ($F > 1$) or
supressed ($F < 1$) spontaneous emission at subwavelength
scale

Strong coupling: Cavity QED

V_m is extremely small → $g (\propto \frac{1}{\sqrt{V_m}})$ is very large
 Q is not high due to loss → Low-light level nonlinear optics

表面等离激元如何介入和量子体系的相互作用？

Weak coupling:

- 1) 在表面等离激元结构的近场区域内为偶极跃迁提供了较强的各向异性Purcell 系数环境（态密度）
- 2) 激发的表面等离激元是局域的电磁波，可以发生在纳米尺度上定域的与原子系统的作用（近场增益）

Strong coupling:

- 3) 量子的表面等离激元与单量子体系的相互作用

本章内容：

5.1 纳米结构近场区域偶极子弛豫系数

5.2 SPP增强分子荧光的前沿进展

5.3 量子的SPP 及其与量子体系相互作用

5.4 我们在交叉领域的几个工作

附录： 分子荧光的知识

5.1 纳米结构附近偶极子弛豫系数

问题的由来：

量子提法：当偶极子放在纳米结构附近或离介质和金属表面很近时，所处的空间局域模式态密度（LDOS）有很大变化，导致其偶极跃迁弛豫系数有很大改变。——态密度的角度

经典提法：导致偶极子的弛豫有两种原因，一种是由于能量辐射到无穷远，叫做辐射弛豫；一种是由于能量耗散到周围的吸收介质中，叫做非辐射弛豫。——能量损失的角度

通常来说，由于纳米结构或者界面的存在会导致decay rate 变大，或激发态寿命变短。表现为荧光谱变宽。但在特殊设计的纳米结构或材料中，有时会使激发态寿命变长。

在无吸收 $\epsilon=n^2$ 介质中的decay rate

自由空间中原子的自发辐射系数: $\Gamma_0 = \frac{\mu^2 \omega_A^3}{3\pi c^3 \hbar \epsilon_0}$

如果场的哈密顿量和电场算符可写成如下形式:

$$\begin{aligned} H &= \frac{1}{2} \int dV (D \cdot E + B \cdot H) \\ &= \frac{1}{2} \int dV (\epsilon_0 \epsilon E \cdot E + \mu_0^{-1} B \cdot B) \end{aligned} \quad \hat{E} = \frac{1}{n} \hat{E}_{\text{free}}.$$

根据fermi's golden rule, 自发辐射系数可写为:

$$\Gamma \propto \int_0^\infty k^2 dk \langle 0 | \hat{E}_j^2(k) | 0 \rangle \delta(\omega_k - \omega_A)$$

在 ϵ 介质的自由空间中, 自发辐射系数是:

$$\Gamma = n \Gamma_0$$

在吸收介质中decay rate的一般表达式（量子）

这时 ϵ 表示为：

$$\epsilon(\omega) = \epsilon'(\omega) + i\epsilon''(\omega) = n^2(\omega) = [\eta(\omega) + i\kappa(\omega)]^2.$$

自发辐射系数的通式为：

$$\Gamma = \frac{2}{\hbar} \operatorname{Im}\{\mu_i G_{ij}(0, \omega_A) \mu_j\}$$

$$\begin{aligned} \Gamma &= \frac{2\pi}{\hbar^2} \sum_f |\langle f | \mu \cdot \hat{E}(r_A, t) | 0 \rangle|^2 \delta(\omega_f - \omega_A) \\ \langle 0 | \hat{E}_i^+(r, \omega) \hat{E}_j^-(r', \omega') | 0 \rangle &= \frac{\hbar}{\pi} \operatorname{Im} G_{ij}(r - r', \omega) \delta(\omega - \omega') \\ \hat{E}(r, t) &= \int_0^\infty d\omega \{ \hat{E}^+(r, \omega) e^{-i\omega t} + \hat{E}^-(r, \omega) e^{i\omega t} \} \end{aligned}$$

激发态分子的弛豫系数的经典定义

先从经典的角度定义辐射弛豫系数和非辐射弛豫系数：

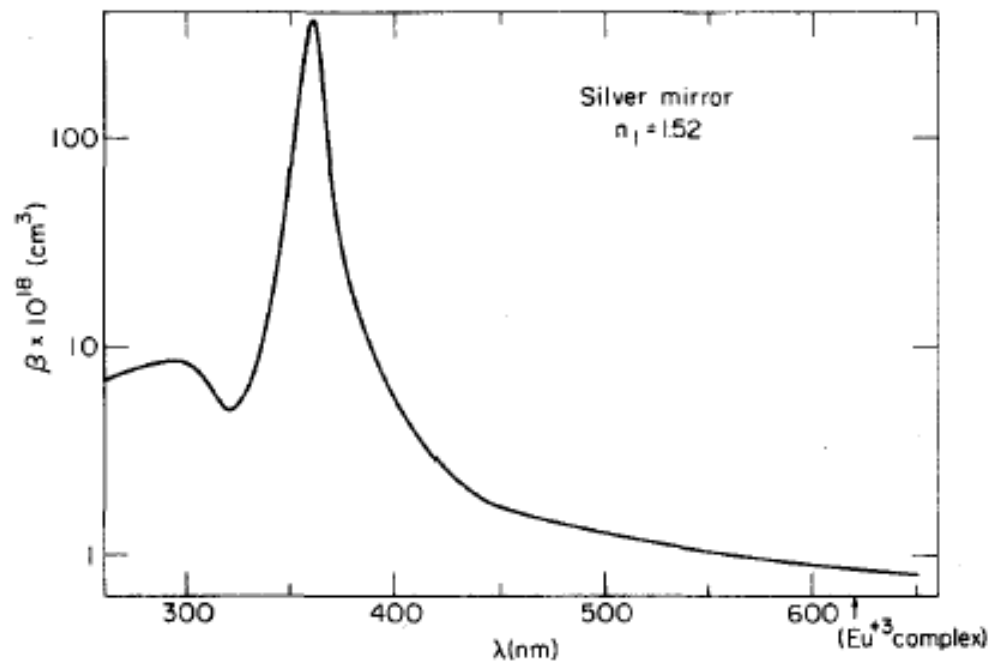
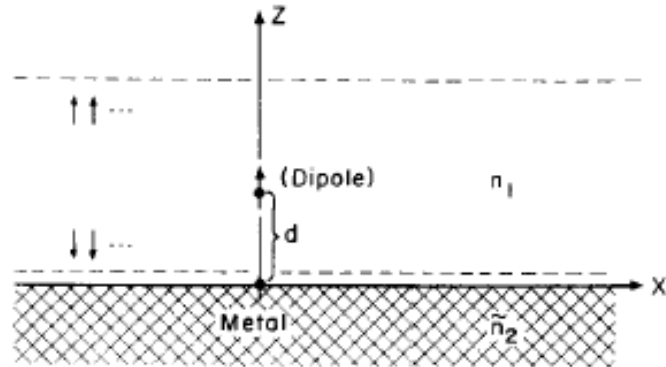
$$\gamma = \gamma^R + \gamma^{NR}$$

$$\gamma^R = \frac{1}{W} \int_{r \rightarrow \infty} d\Omega \ r^2 \vec{S} \cdot \hat{n} \quad \gamma^{NR} = \frac{1}{2W} \int_V d\tau \ \sigma |\vec{E}|^2$$

参数设置

where $\vec{S} = (c/8\pi) \operatorname{Re}(\vec{E} \times \vec{H}^*)$ is the Poynting vector, σ is the conductivity of the substrate, W is the average energy of the dipole, $d\Omega$ is the differential element of the solid angle, and $d\tau$ is the differential volume element. The integral in eq 2 is over a surface at infinity while that in eq 3 is over the volume of the dissipative substrate.

平板金属附近激发态分子的弛豫



几点说明：同等距离下，偶极子在垂直于界面时的弛豫系数大于平行的情况。离界面越近，弛豫越大，即分子激发态寿命越短。弛豫系数随波长有明显变化关系，通常认为和表面等离激元有关。

金属薄膜附近激发态分子的弛豫

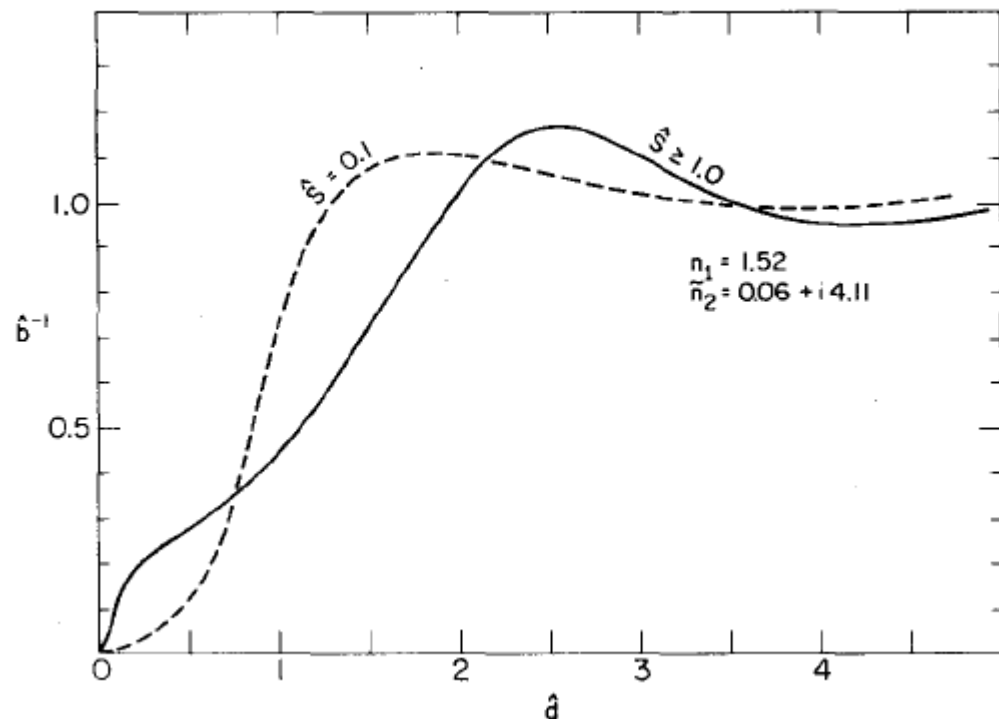
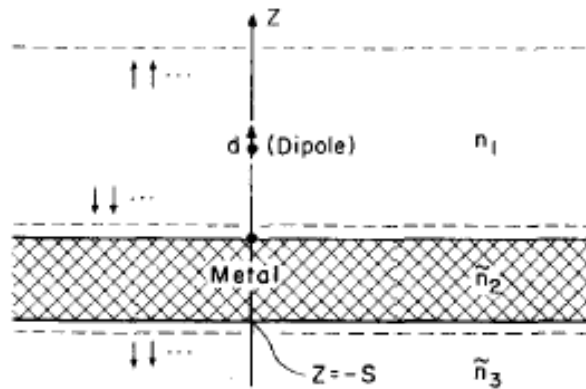
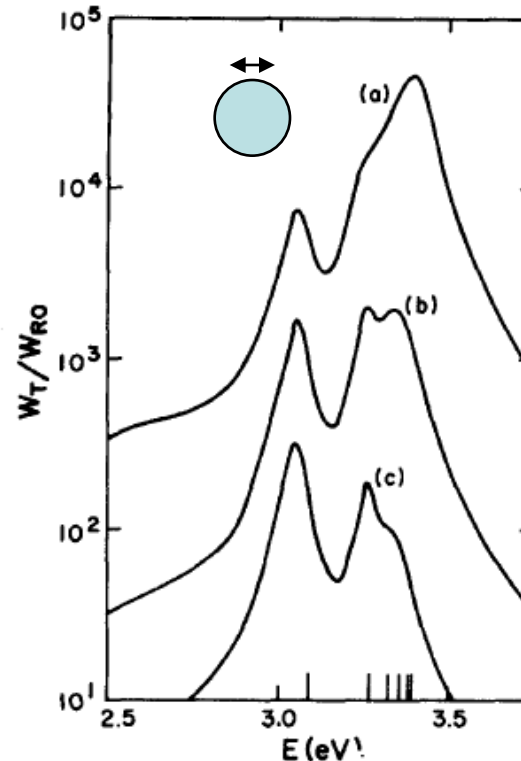
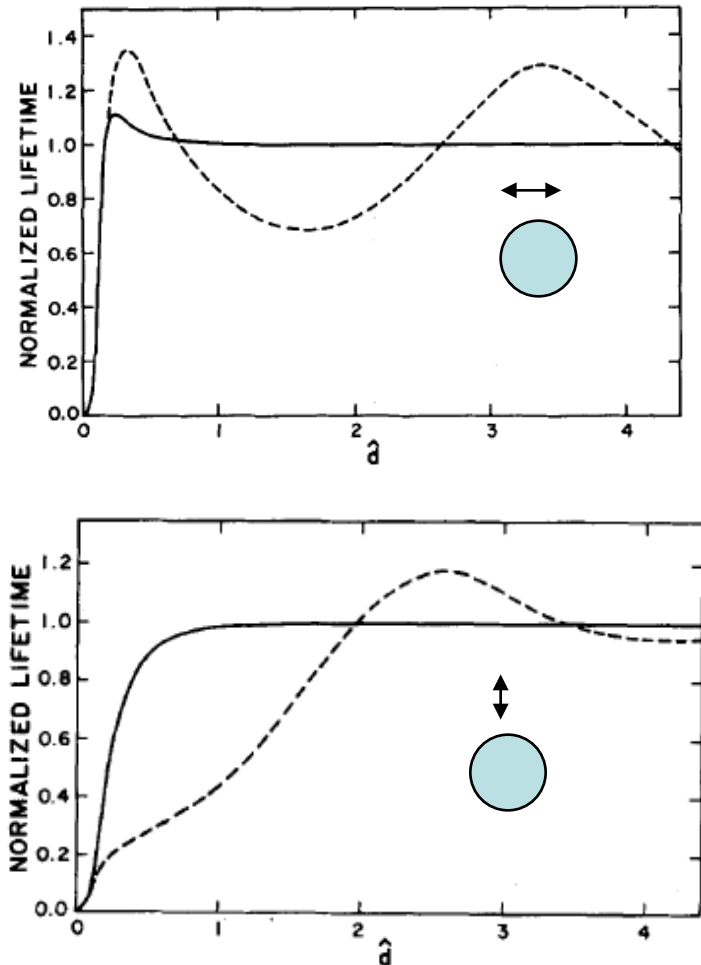


FIG. 5. The effect of the thickness of the metal mirror on the

说明：上图给出了偶极子寿命随金属膜厚变化的曲线。实线代表平板金属的结果。金属膜厚度对激发态寿命影响很大，在膜很薄时，激发态寿命更短。

金属小球附近激发态分子的弛豫



参数：波长612nm，半径10nm银小球，左图距离小球10nm，上图距离小球分别是2nm,5nm,10nm. $d=.15$ 相当于60nm远。虚线是平板情形。

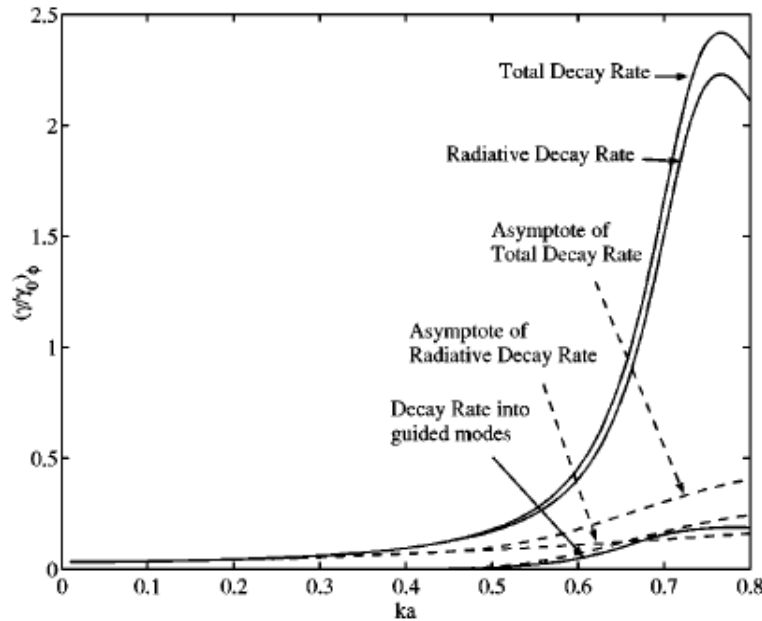
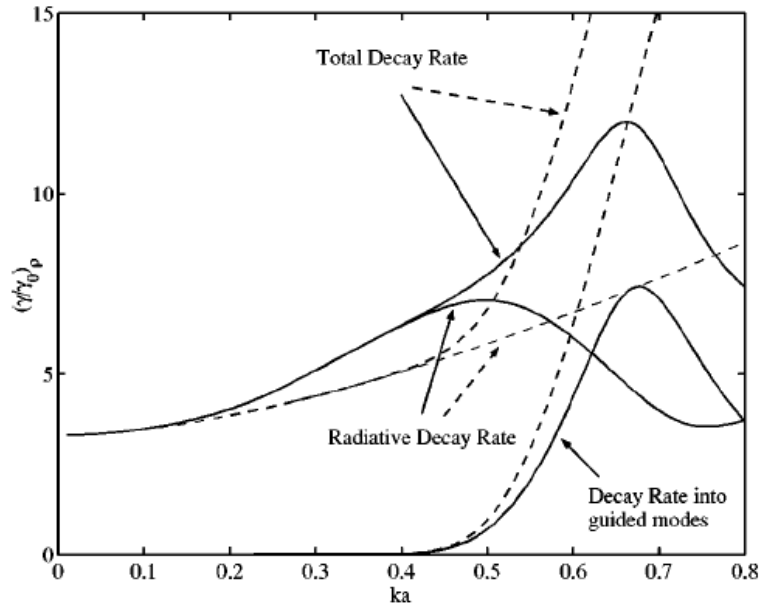
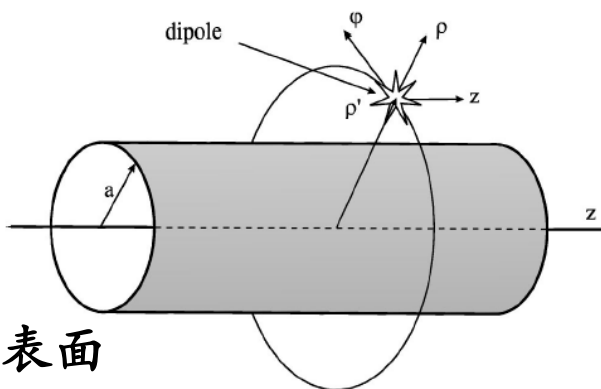
结论：离小球越近，分子的寿命越短。垂直情况下，距离很近时，相对于平板金属来说，寿命变化更快；平行情况下，距离远时，平板金属影响更大。

纳米光纤附近激发态原子的弛豫

虚线：准静态近似结果

左下图： ρ 方向偏振的偶极子， z 方向同

右下图： φ 方向偏振的偶极子，偶极子在表面

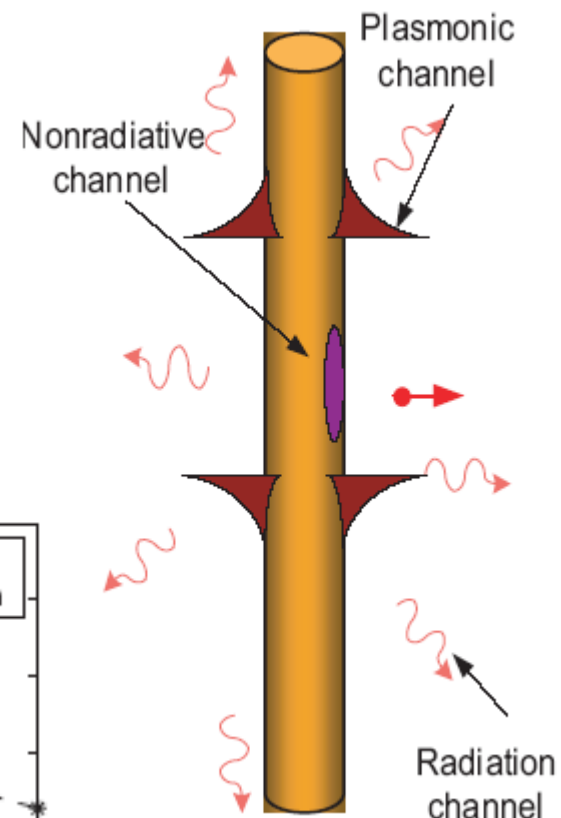
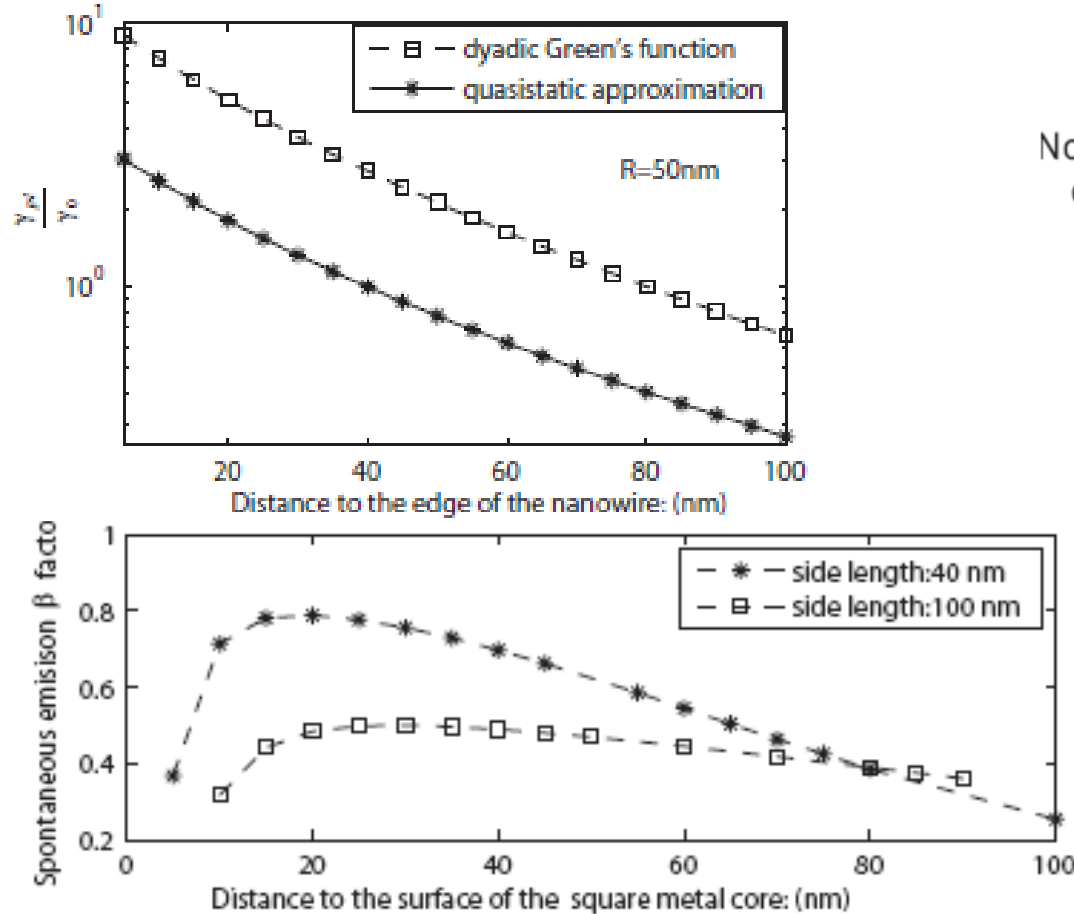


发现：当光纤半径较小时，辐射弛豫为主，与准静态近似结果相符。半径略小于波长时，波导模式的弛豫贡献很大， ρ 和 z 方向偏振的偶极子弛豫增大更显著，可以有效激发波导模式；而 φ 方向偏振的偶极子与波导模式的耦合效率很小。

Spontaneous emission rate of an excited atom placed near a nanofiber

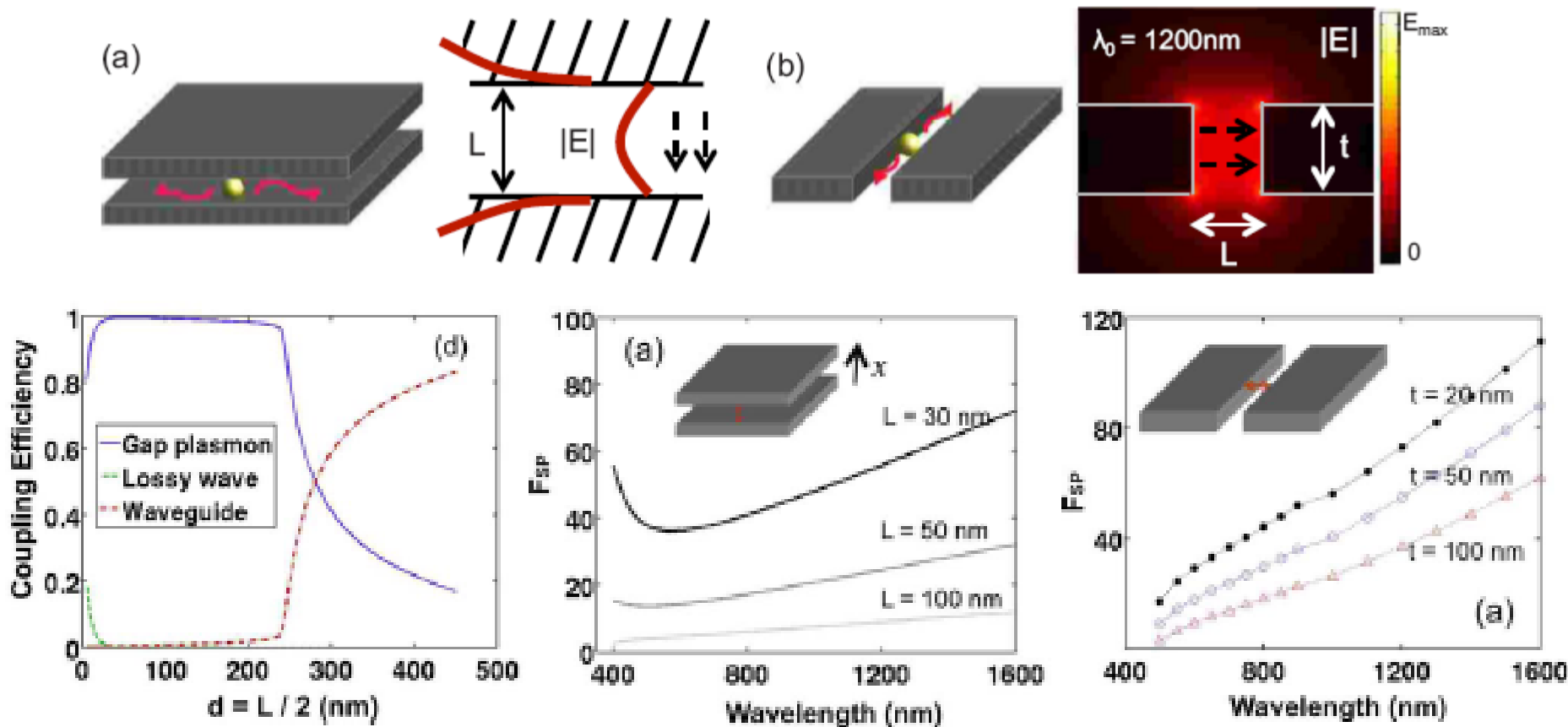
V. V. Klimov et al, PRA, 69,013802 (2004) 。

纳米金属线附近激发态原子的弛豫



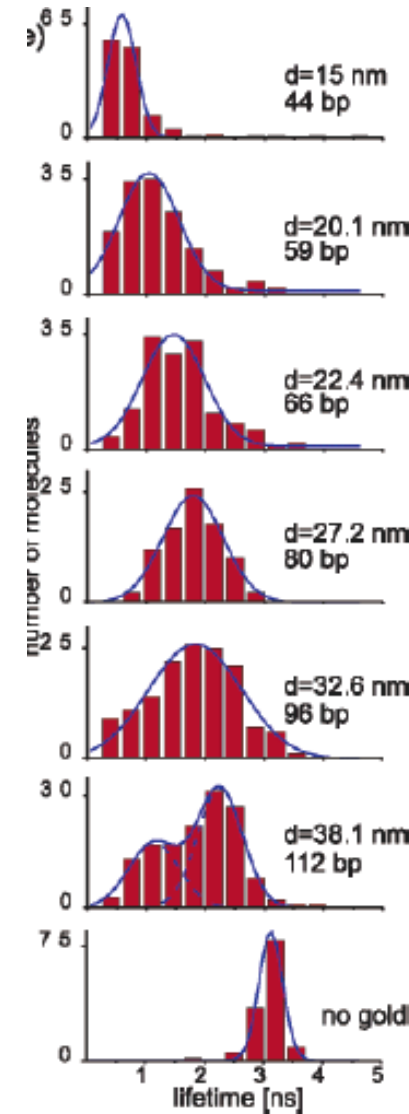
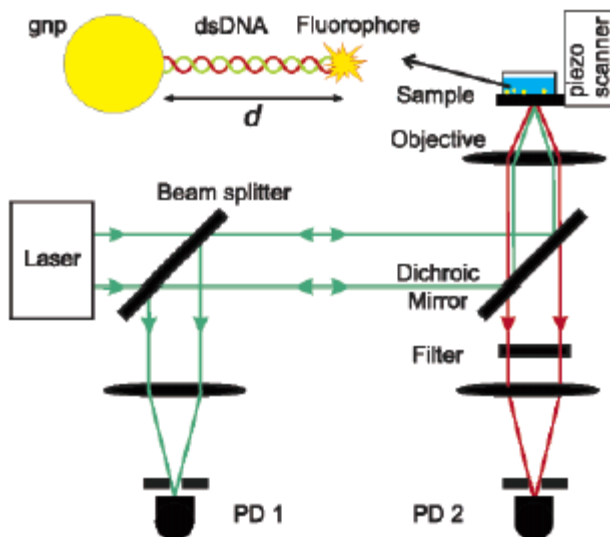
发现：偶极子越接近纳米线，SP弛豫越大，而SP耦合效率在距离非常小时有下降。纳米线半径减小，SP弛豫增大。选取合适的边长和距离，方形sp波导的耦合效率也可以达到80%。

MIM型SPP波导中激发态原子的弛豫



发现：MIM波导中SP弛豫占主导。MIM slab间隔减小，或MIM slot厚度减小，群速度和模体积减小，因此弛豫增大。在较宽的波长范围内，MIM波导对弛豫有很大的非共振增强。

激发态分子寿命可做为“纳米尺子”



发现：金纳米小球影响分子辐射和淬灭的过程，从而影响分子的寿命。测量分子寿命可以作为纳米尺子。15 nm直径的金球在15-25 nm距离范围灵敏度最好。改变金球的直径，可以调节量程和灵敏度。

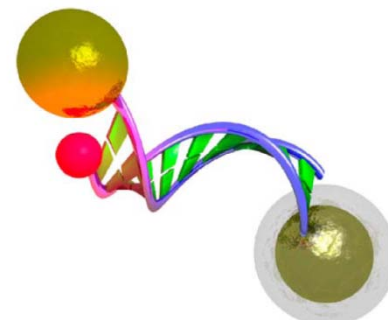


5.2 SPP增强分子荧光的前沿进展

SPP发生时，纳米结构附近的巨大近场增益在非线性光学、拉曼光谱、分子荧光、纳米器件、光场囚禁等方面有广泛应用。

纳米金属结构附近量子发射体系的讨论中，近场增益和decay rate增益是互相博弈的。

基本现象：用SP控制分子和量子点的发光行为；纳米金属颗粒周围的场增强效应，影响荧光强度，寿命以及谱分布；金属纳米颗粒附近的染料分子荧光淬灭、荧光谱变化，及Forster能量传递；单个分子耦合到纳米天线控制辐射方向等。



Plasmonic结构控制分子荧光的原理图

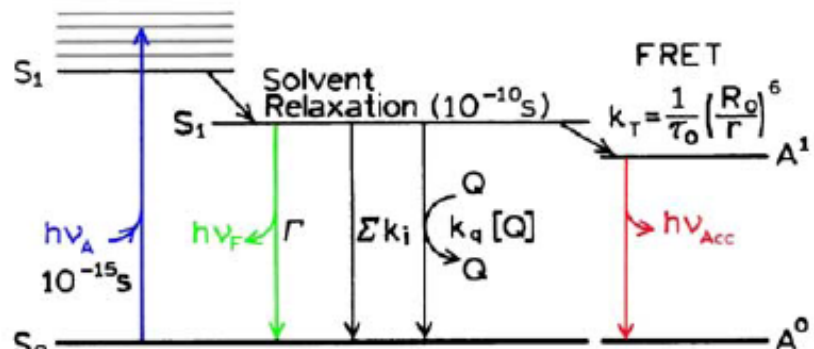


Figure 1. Free-space emission.

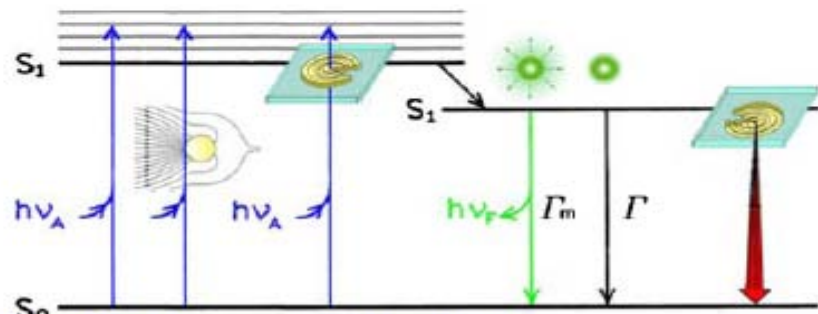
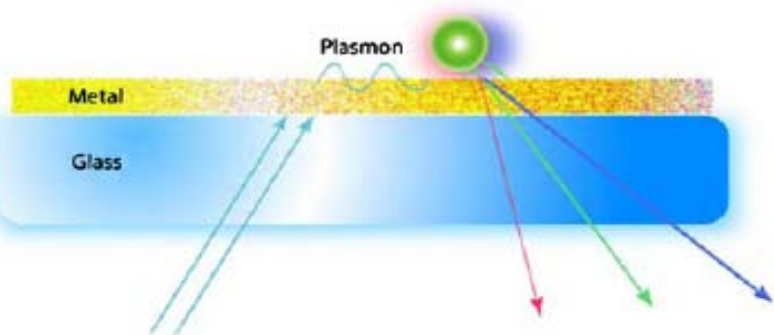


Figure 2. Plasmon controlled emission.

可以看到：主要从两个方面参与作用，利用表面等离激元近场增益增加吸收，另一方面，通过增加非辐射弛豫控制谱线宽度及激发态寿命。

纳米体系近场区域对荧光分子寿命的影响

如右图所示装置中，分子感受到的光场：

$$\mathbf{E}_{\text{mol}}(\mathbf{r}, \omega) = \mathbf{E}(\mathbf{r}, \omega) + \mathbf{S}(\mathbf{r}, \mathbf{r}_m, \omega) \cdot \alpha^{\text{eff}}(\omega) \cdot \mathbf{E}_{\text{mol}}(\mathbf{r}_m, \omega)$$

with

$$\alpha^{\text{eff}}(\omega) = \alpha_0(\omega) \cdot \mathbf{M}(\mathbf{r}_m, \omega).$$

$$\mathbf{M}(\mathbf{r}_m, \omega) = [\mathbf{I} - \mathbf{S}(\mathbf{r}_m, \mathbf{r}_m, \omega) \cdot \alpha_0(\omega)]^{-1}.$$

可以看到：随着分子与银膜距离的减小，近场增益变大，同时，分子弛豫变大，在200纳米内分子寿命衰减很快。这个工作的意义在于：设计了实际的探测系统，并强调近场的作用。

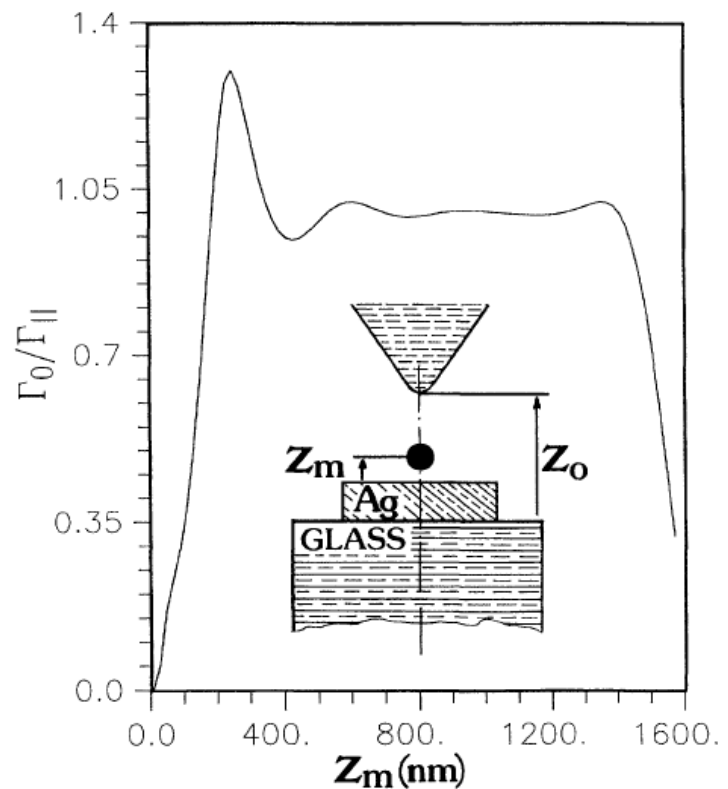
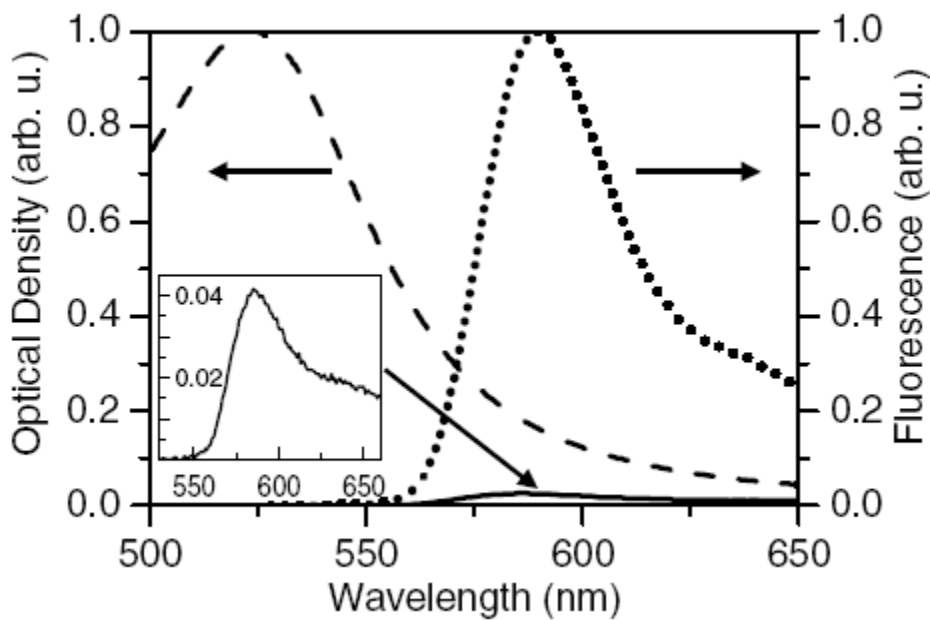
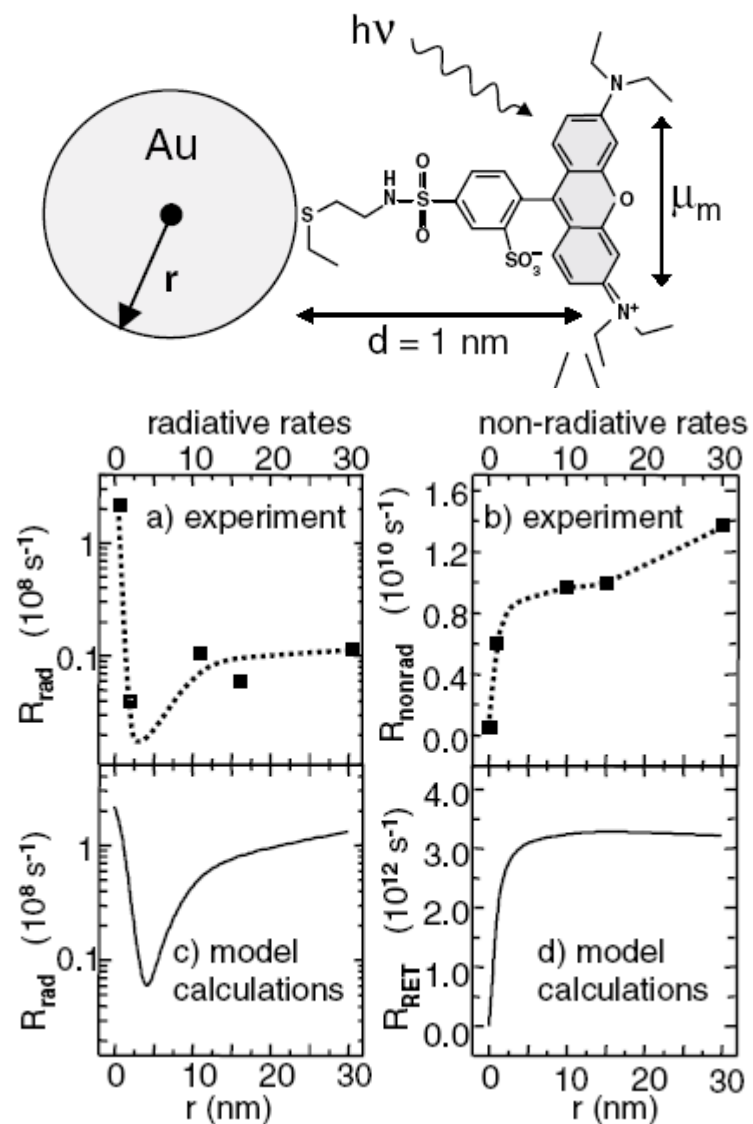


FIG. 2. Distance dependence of the normalized lifetime $\Gamma_0/\Gamma_{\parallel}$ inside the junction, as a function of the position of the molecule. The geometry used in the simulation is described in the inset and the tip-sample separation is maintained at $Z_0 = 1600$ nm. The glass sample is covered with a square shaped silver layer 300 nm long and 20 nm high.

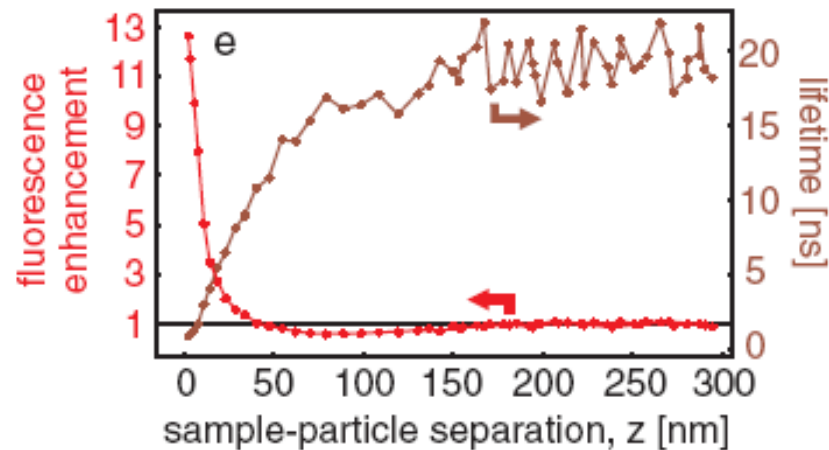
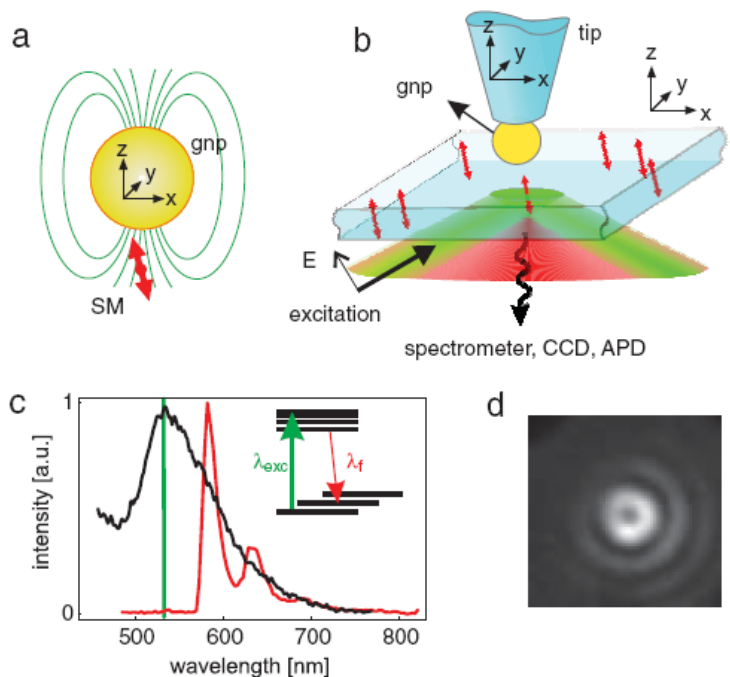
纳米金球附近分子荧光的淬灭：辐射和非辐射弛豫的影响



可以看到：当染料分子靠近15纳米半径的金球时，荧光淬灭近20倍，主要有辐射和非辐射弛豫两个途径。从右图可看出，当金球很小时，辐射弛豫起主要作用，当金球大时，非辐射弛豫主导。



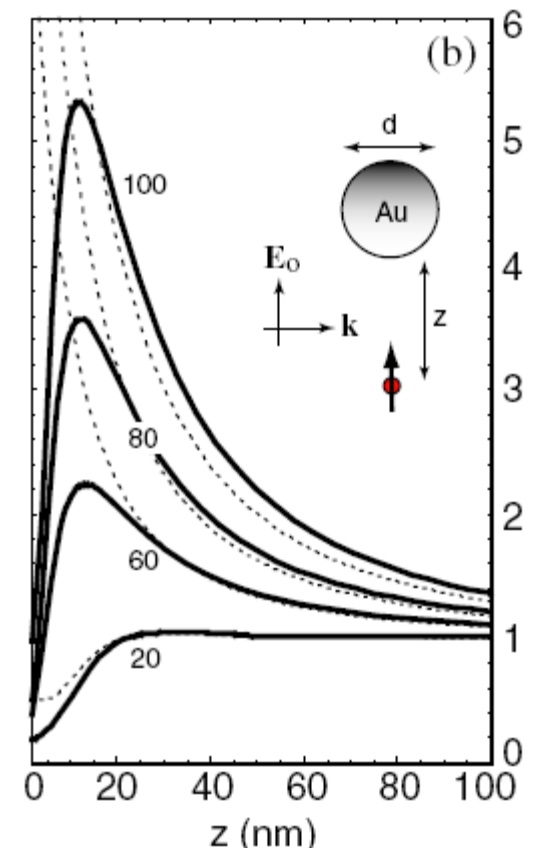
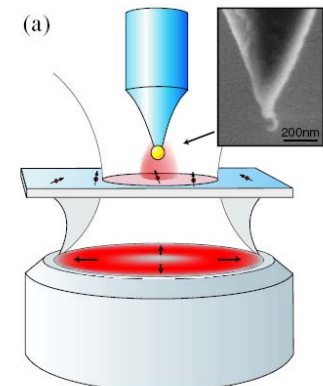
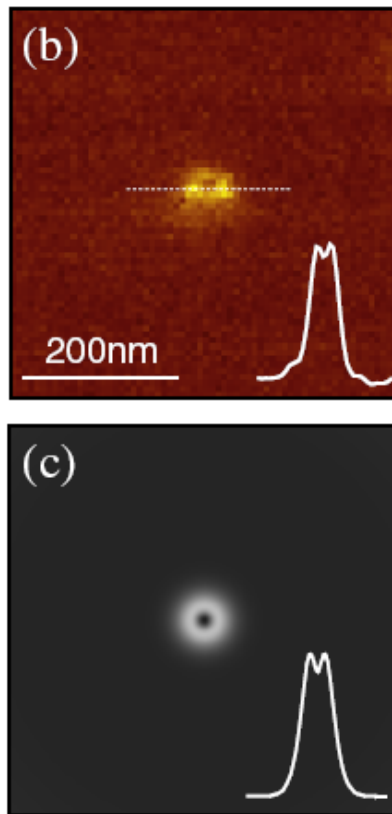
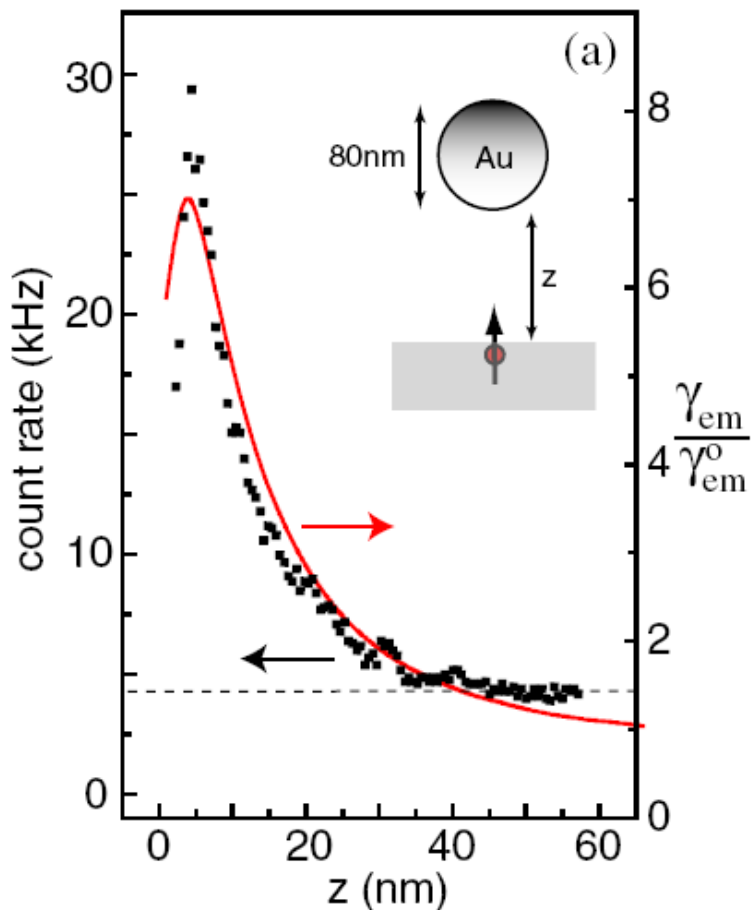
纳米金球颗粒增强单分子荧光



左图：实验装置示意图及分子光谱

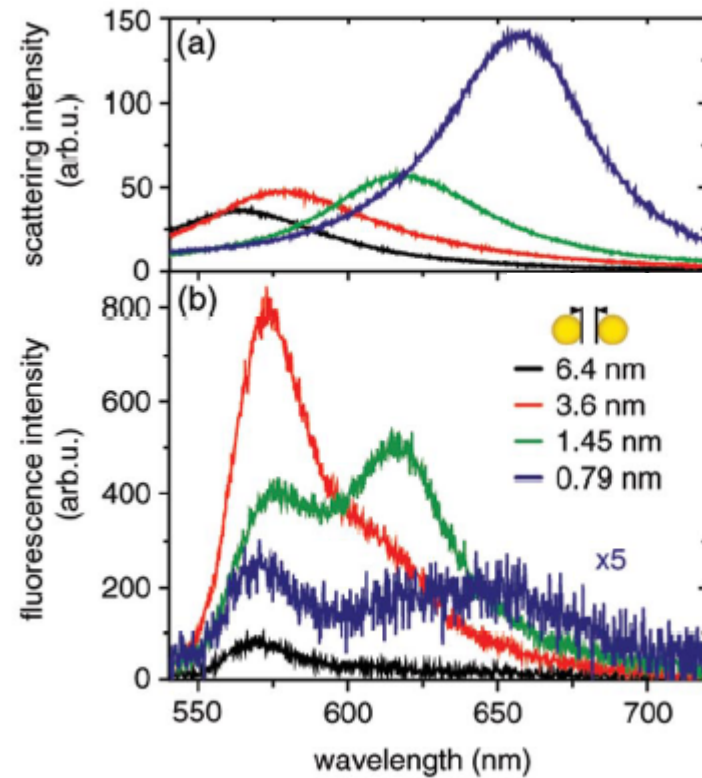
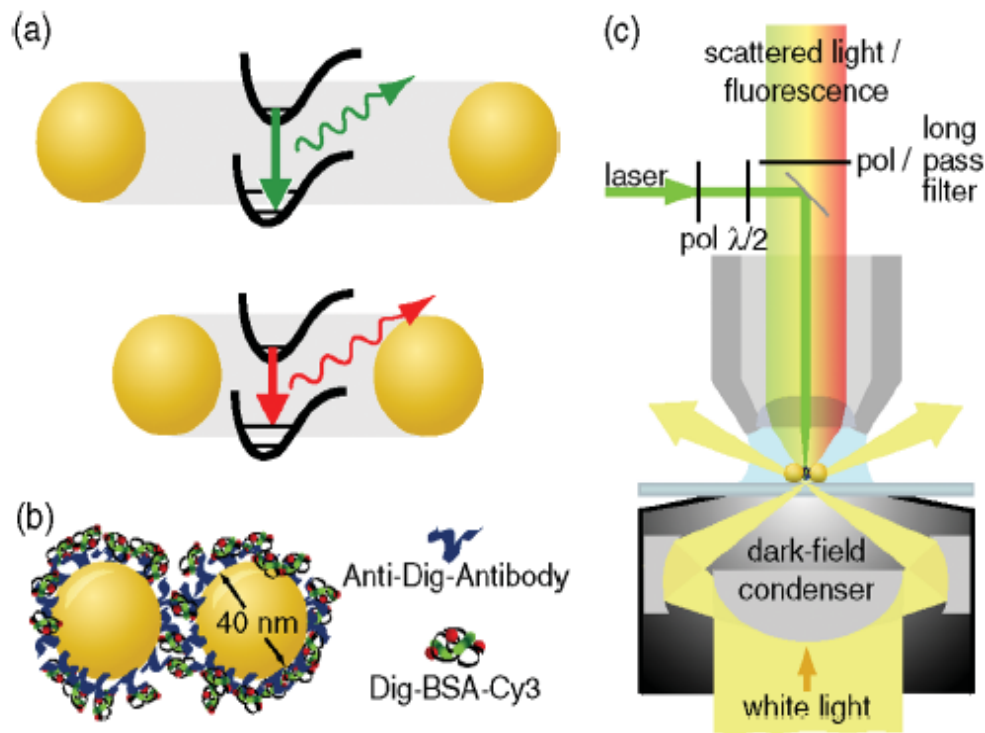
右图：随tip和分子间距离变化，荧光和寿命的增益系数。

纳米金球附近分子荧光从增益到淬灭的连续变化



可以看到：当纳米金球接近荧光分子的过程中，荧光的弛豫发生巨大变化，同时我们可观察到距离变化过程中，荧光从弱到强又到弱的连续变化过程。

通过纳米金球间距离控制荧光谱的形状

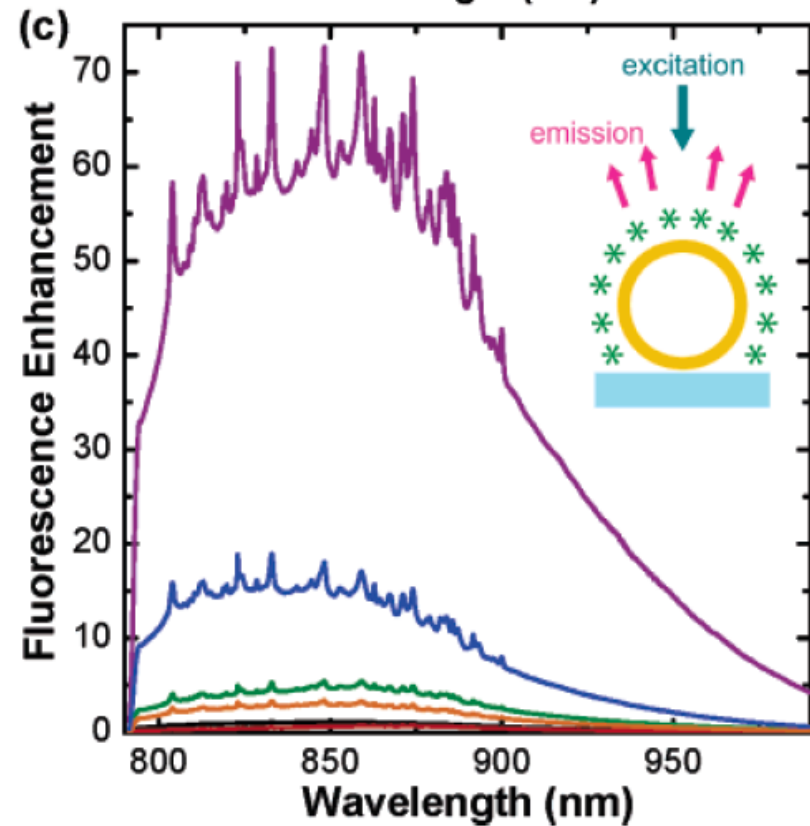
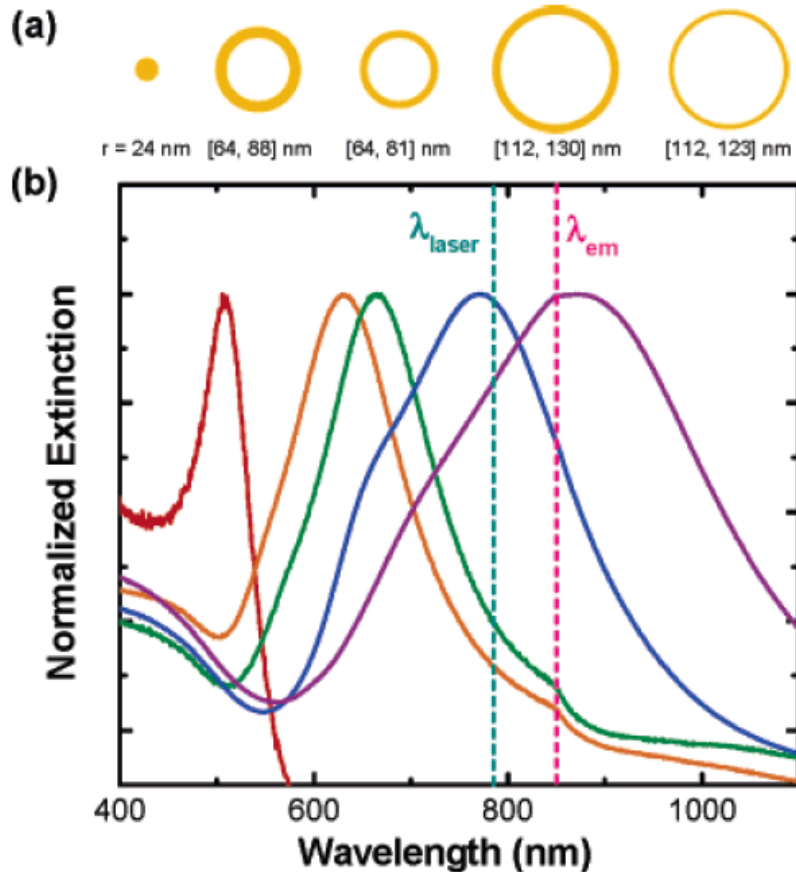


上图：实验装置及原理示意图。

右上图：纳米金属颗粒随其间距离变化的散射谱，可以明显看到，随距离变小，共振红移，**SPR**在起作用。

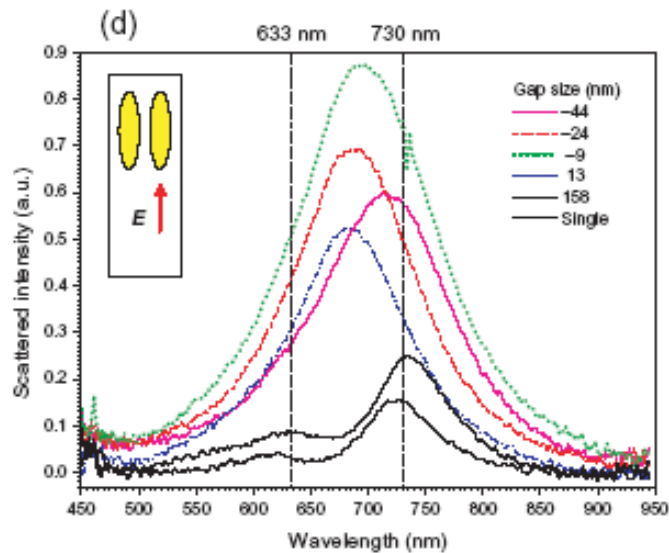
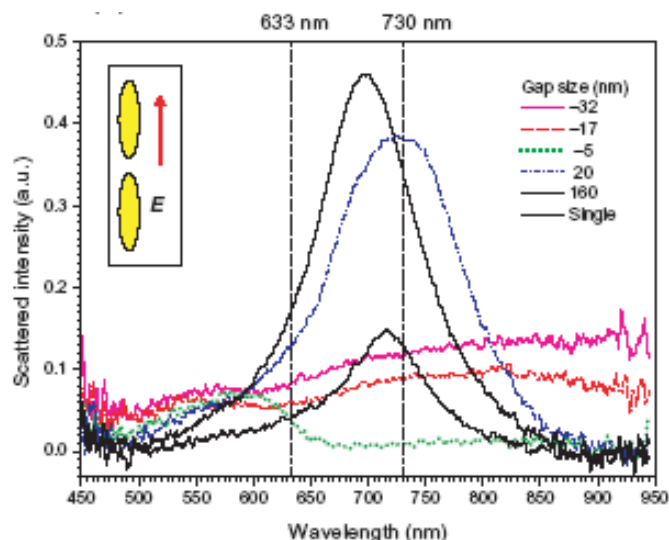
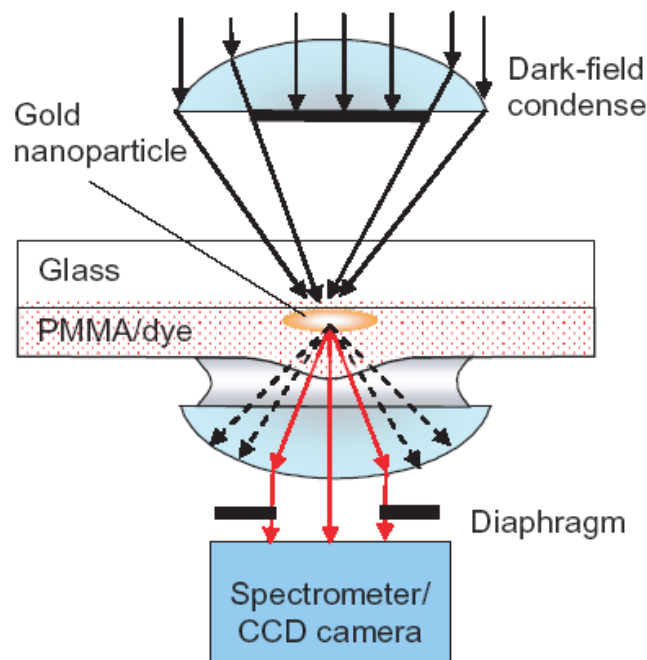
右下图：分子荧光的光谱，其峰值及宽度可由金球间距离调节。

利用金属纳米球壳实现荧光增益



这里为了说明：不仅是纳米金属球， 纳米金属球壳也可用于分子荧光实验，并且显示出更好的可调性。

纳米金棒dimer对荧光的影响

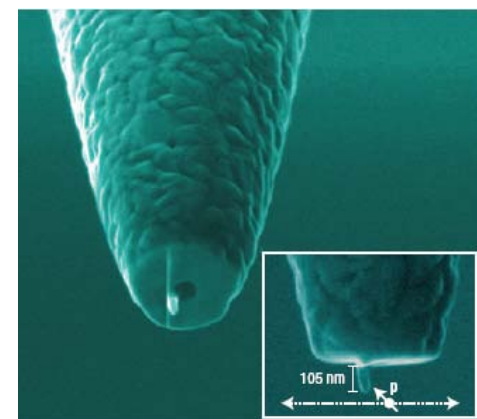
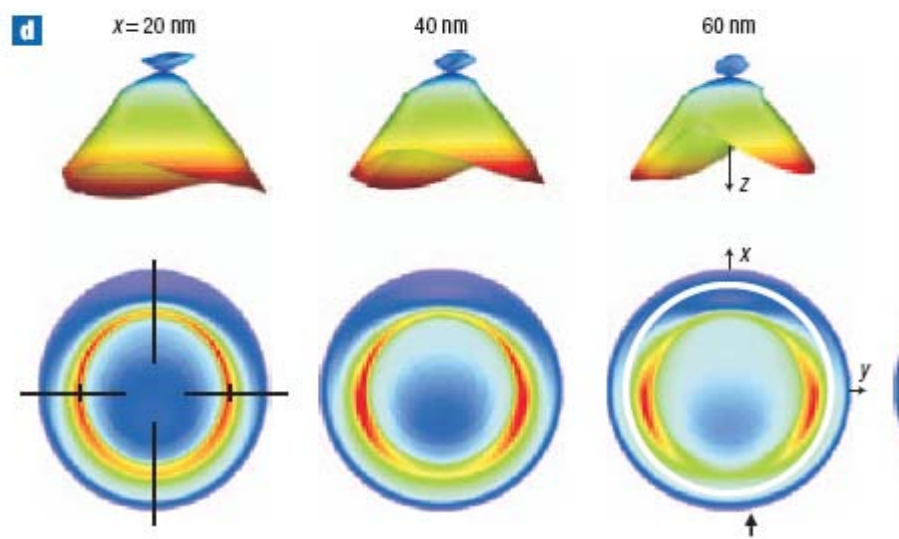
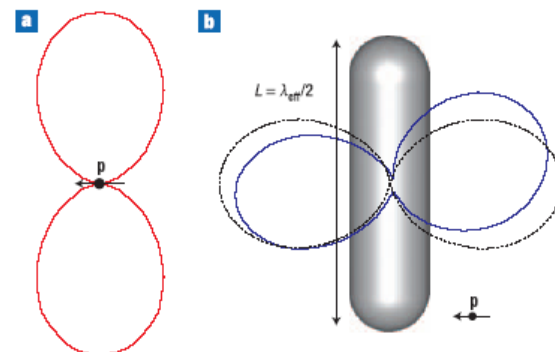
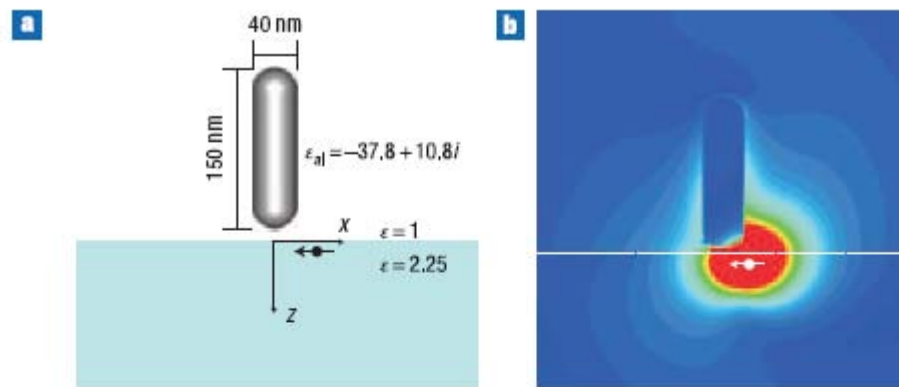


发现：当金棒间距离发生变化时，右边两种情况的SPR的强度发生变化，荧光随之变化。

Fluorescence enhancement through modified dye molecule absorption associated with the localized surface plasmon resonances of metallic dimers ,

George Zoriniants and William L Barnes, New Journal of Physics 10 (2008) 105002.

纳米天线控制荧光发射方向



右上图：偶极子发出的光被纳米天线收集并沿天线方向传走

右下图：铝纳米天线的SEM图

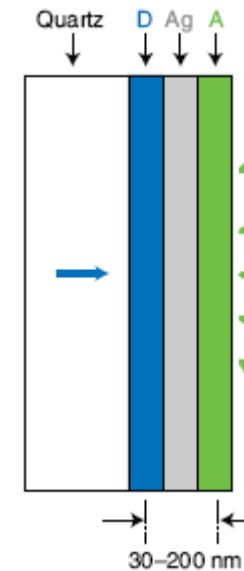
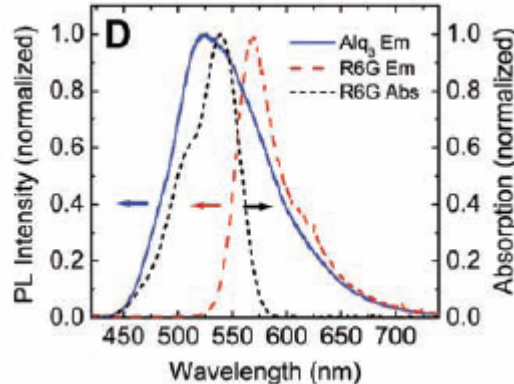
左图：可以看到随距离x的变化， 荧光收集情况。

Forster Energy Transfer Across a Metal Film

W. L. Barnes et al, 2004 (第一章用过)

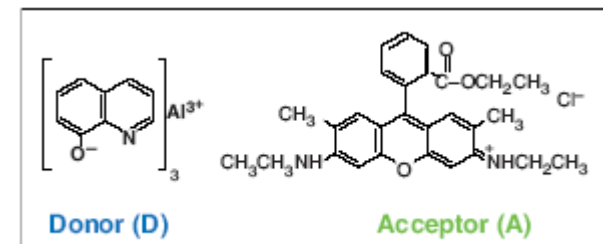
Application work
Molecular plasmonics

Aim to: realize the Forster energy transfer between donor and acceptor across silver film

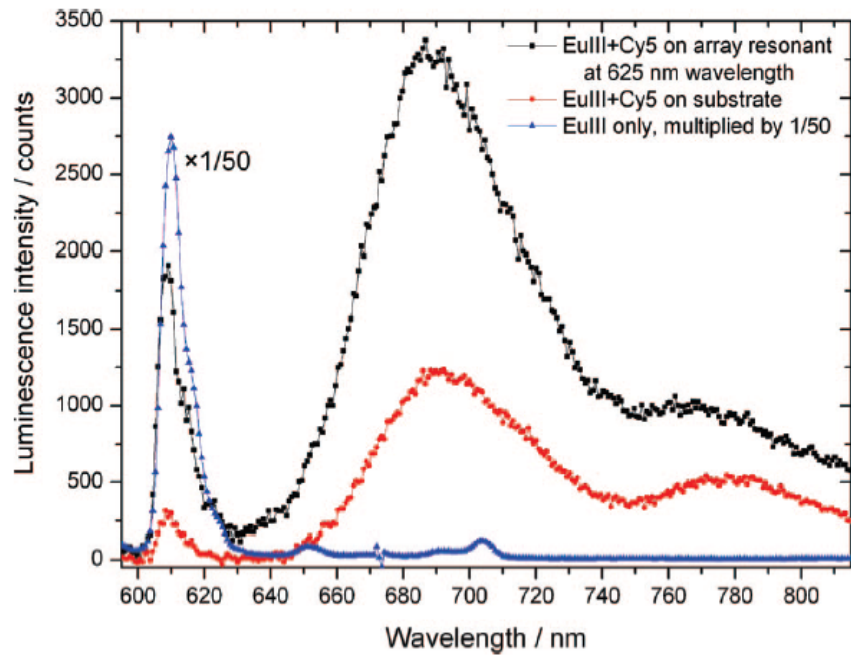
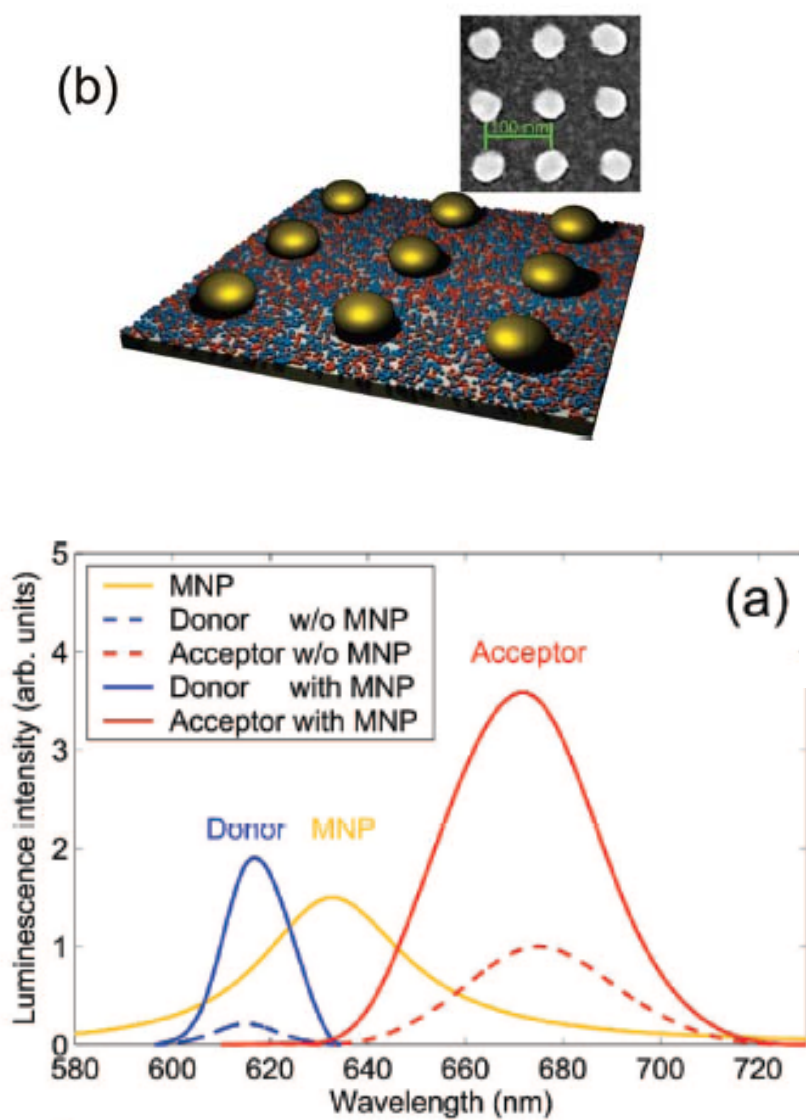


Significance:

toward the realization of an active plasmonic device by combining thin polymer films with thin silver films



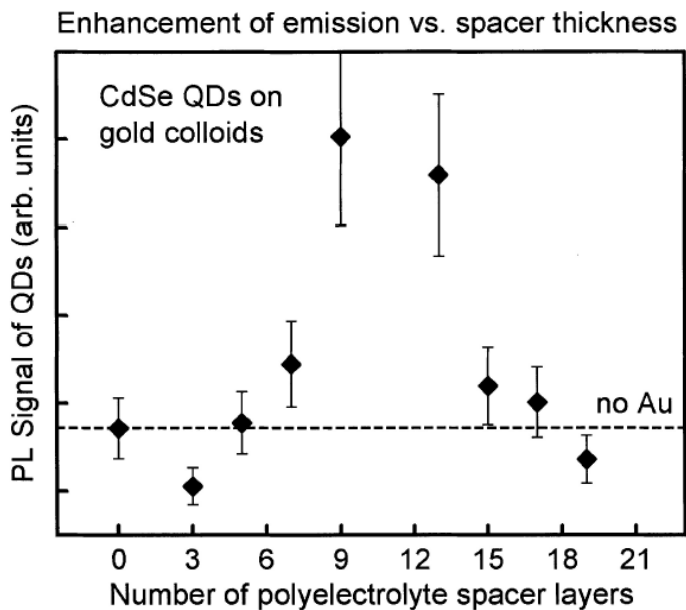
借助于金属颗粒的Forster能量传递



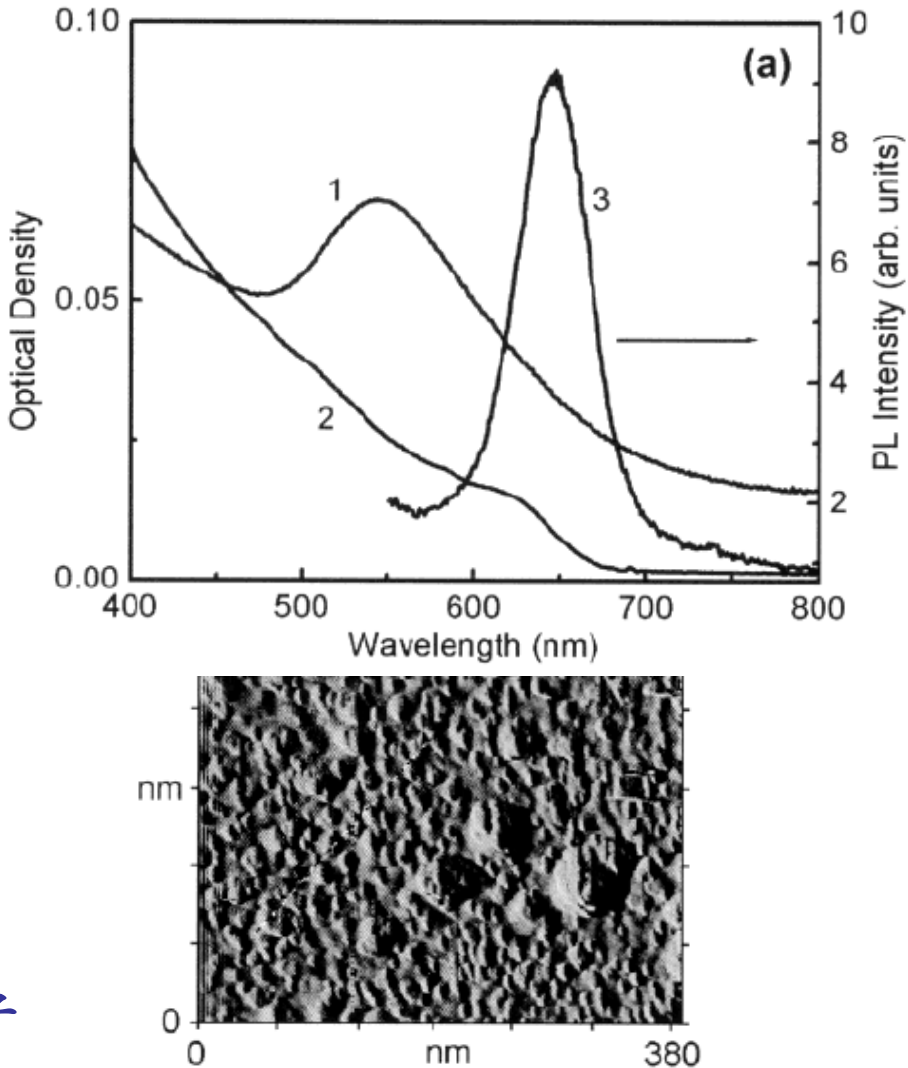
可以看到：将金属颗粒的共振峰设计在acceptor的吸收峰附近，那么从上图可以看到，受体分子的发光被大大增强。

纳米金胶体对量子点发光的增强效果

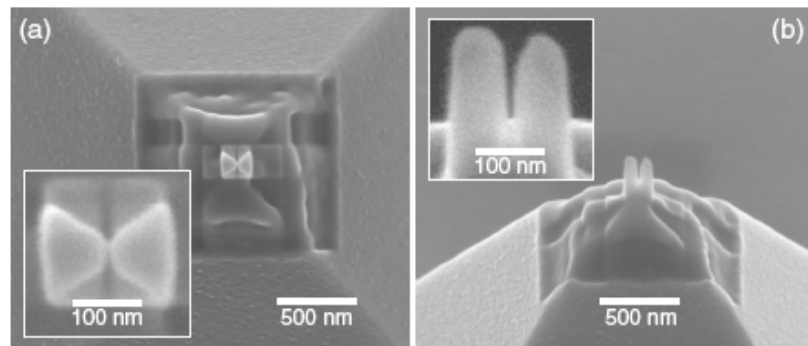
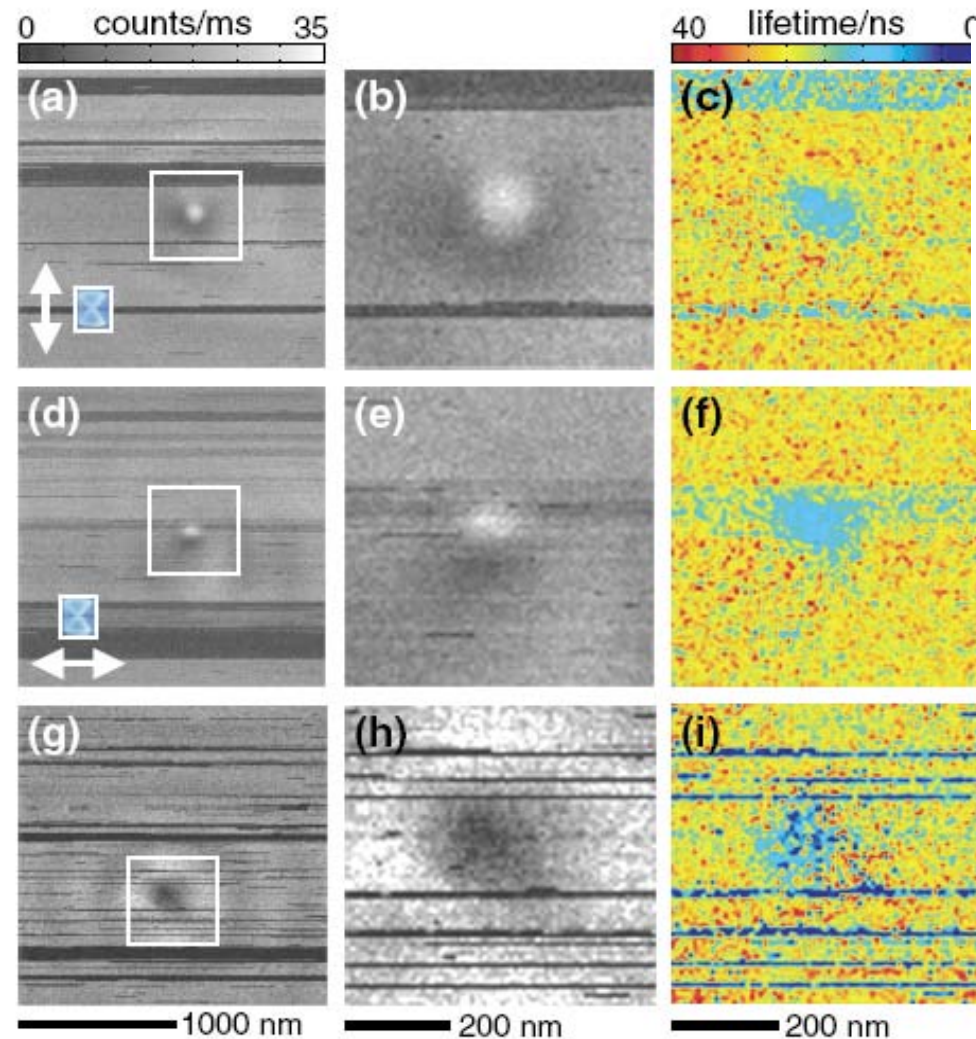
说明：线1是金的吸收谱，2是量子点的吸收谱，3是量子点发光谱。金颗粒的顶端半径10纳米。



可以看到：由于金胶体的存在，量子点发光增强，说明是SPP的作用。



领结型纳米天线激发量子点

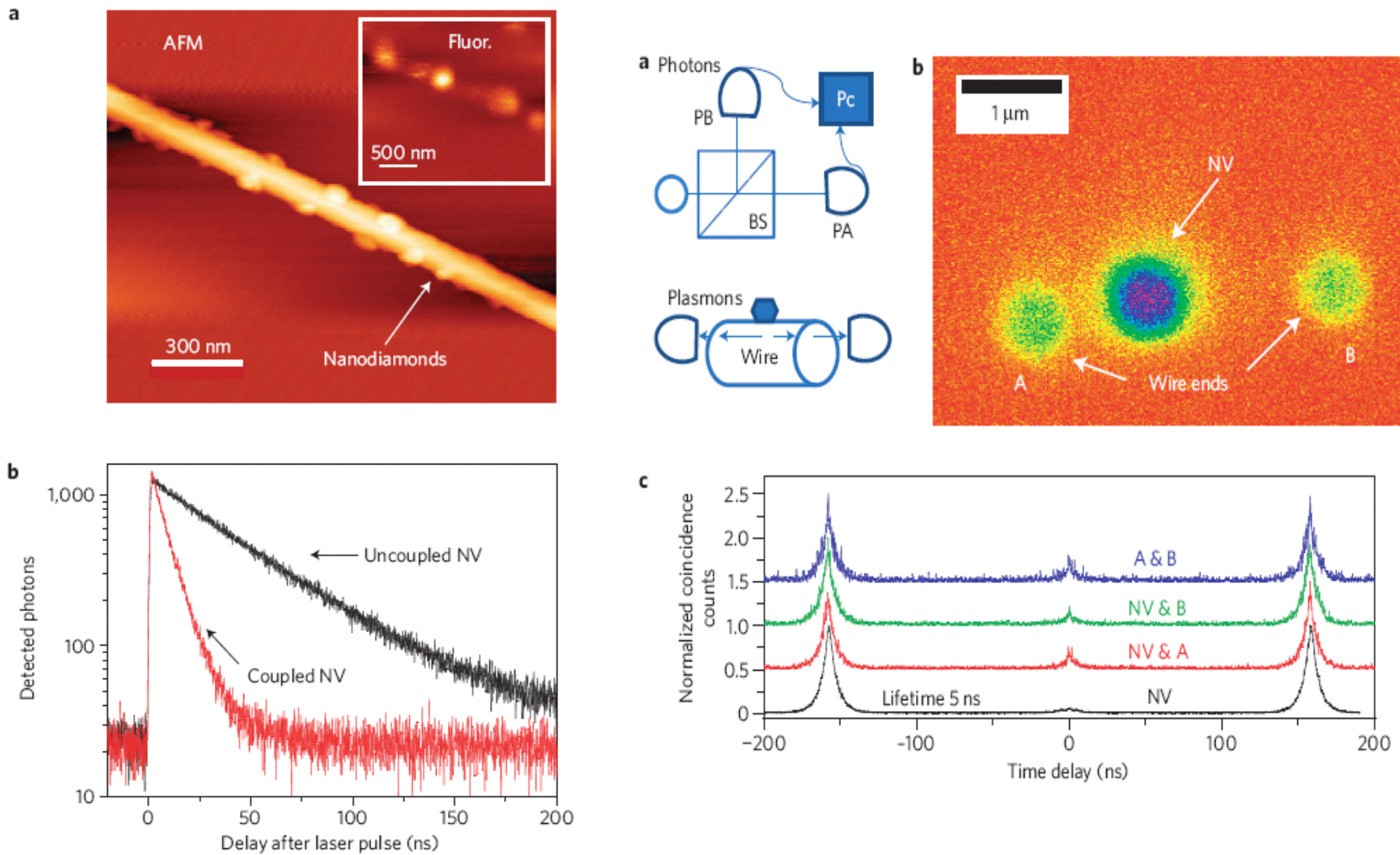


可以看到：制备出的170纳米左右的铝纳米天线，共振激发后，天线附近量子点发光增强，激发态寿命变短。在平行或垂直激发时，情况不同，平行激发后的量子点发光更强，寿命更短。



5.3 量子的SPP 及与量子体系相互作用

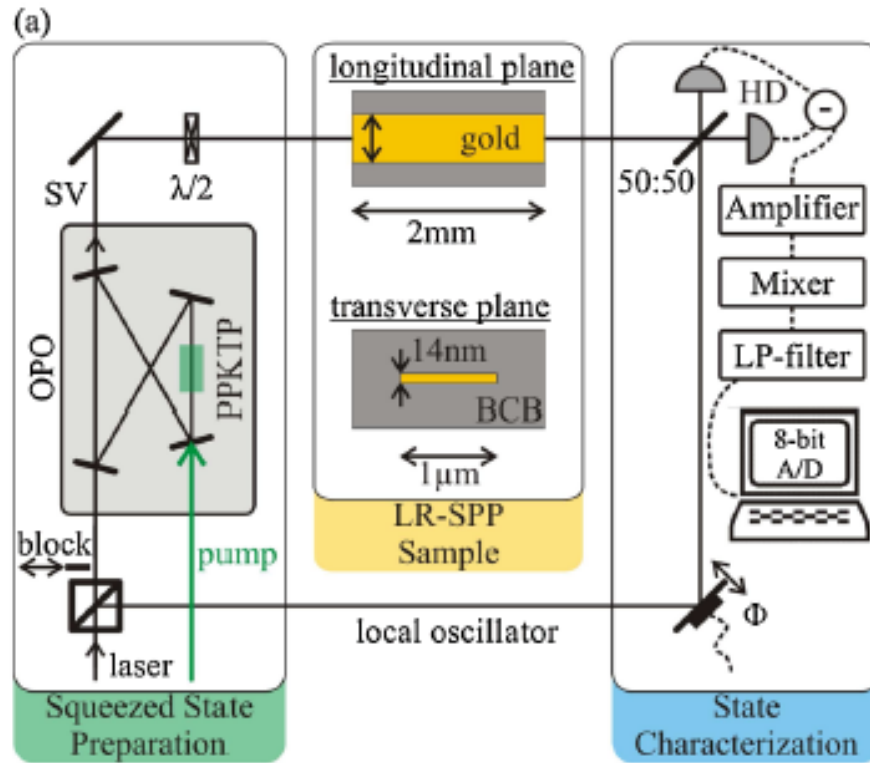
SPP的波粒二象性



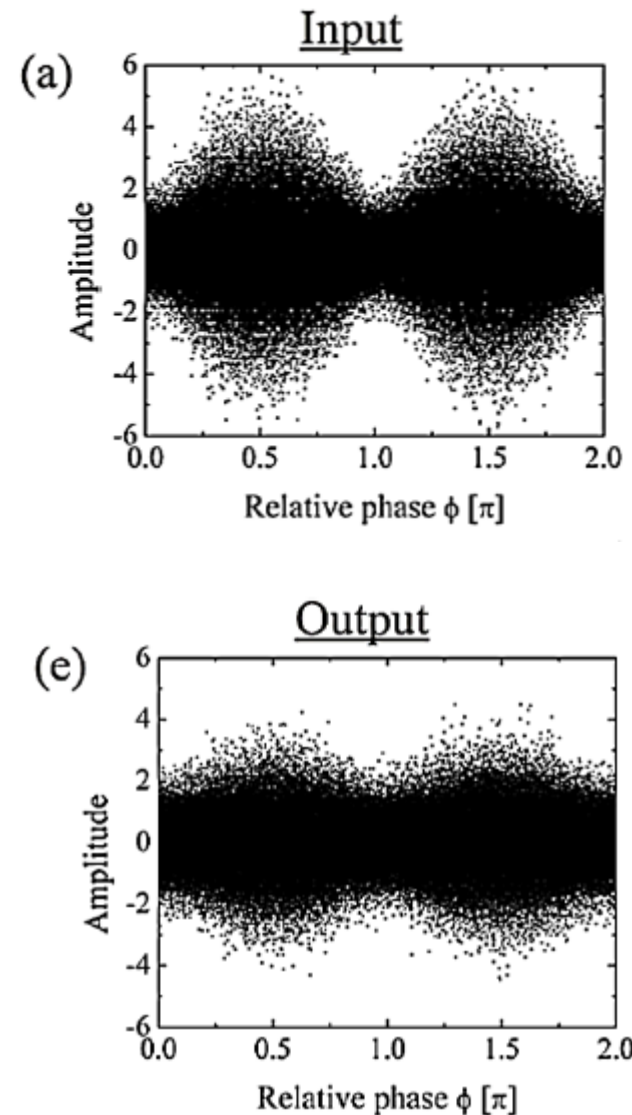
Wave-particle duality of single surface plasmon polaritons

Roman Kolesov et al, nature physics, 5, 470 (2009)

在金纳米线中的压缩态SPP

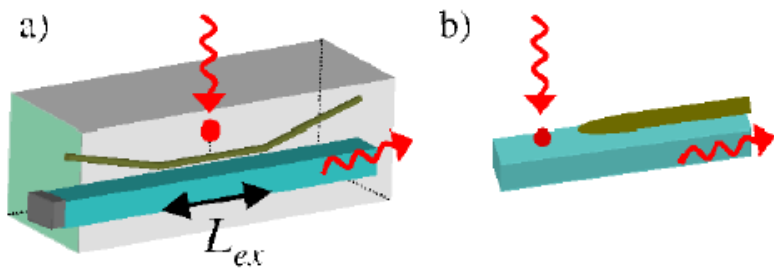


实验装置图及通过纳米金线之前和之后压缩态光场测定。可以看到：由压缩态到SPP再到压缩态的过程。



表面等离激元协助下的单光子源

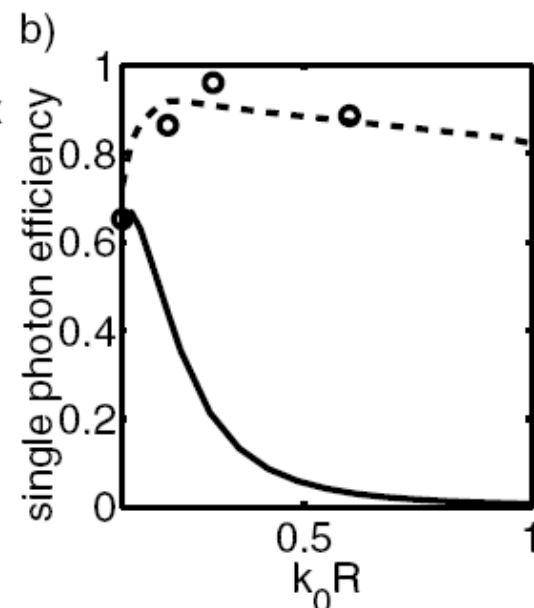
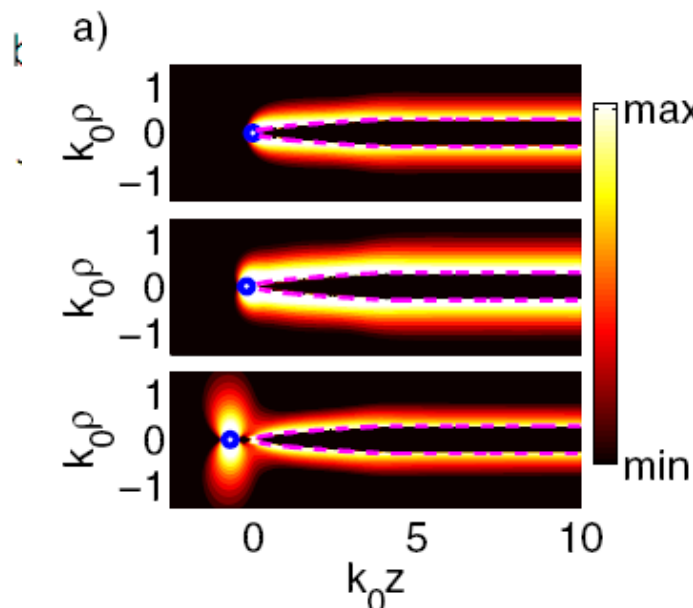
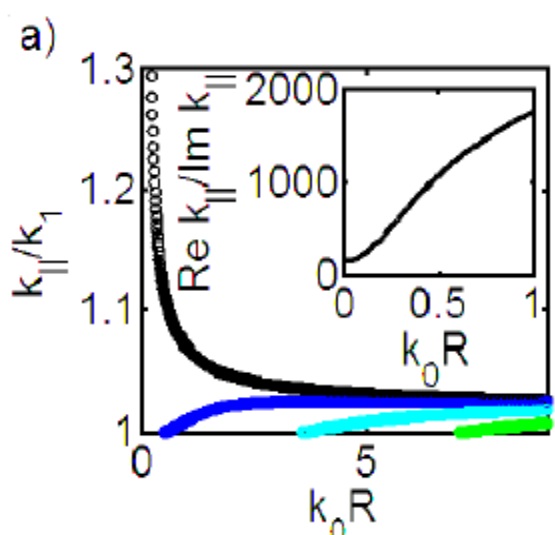
装置包括：量子散射体、纳米金属线和介质波导



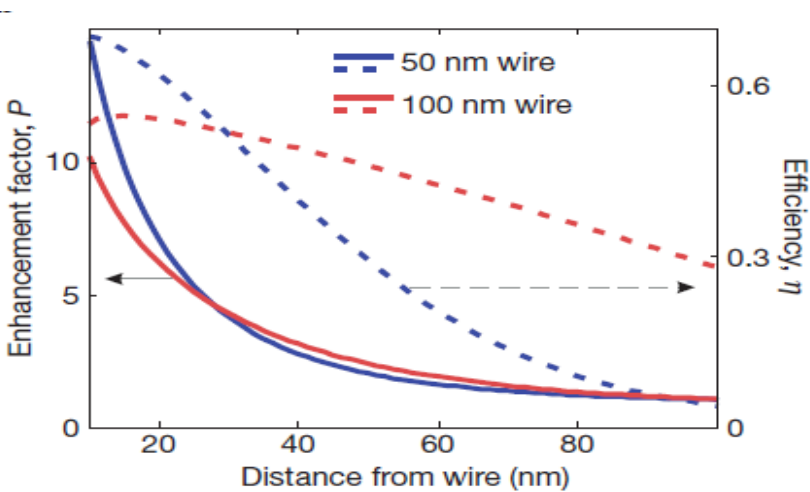
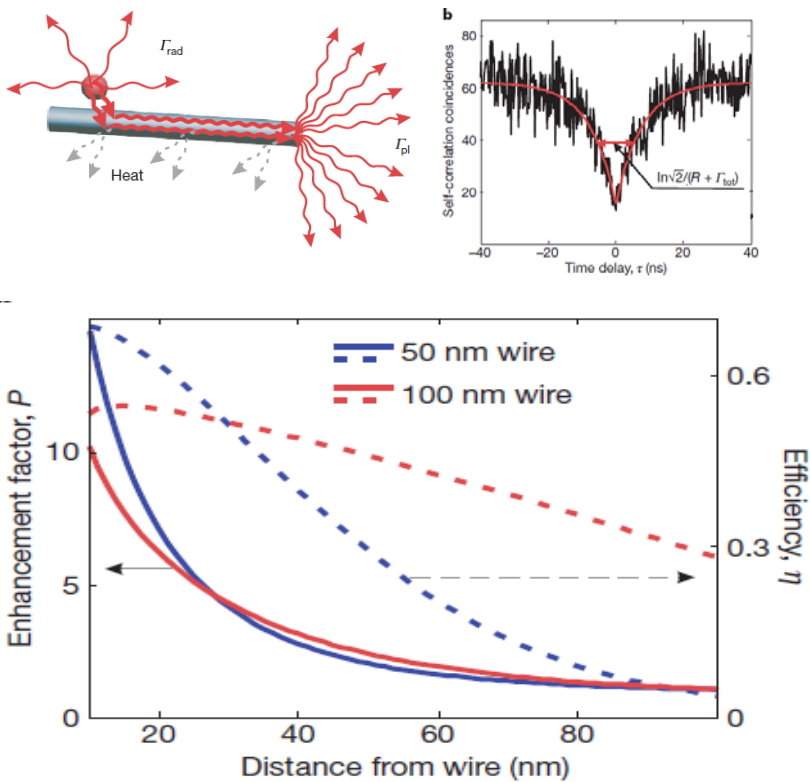
左下图：银线中的SPP模式

中下图：1是非辐射decay主导；2是耦合较好的情况；3是辐射decay主导。

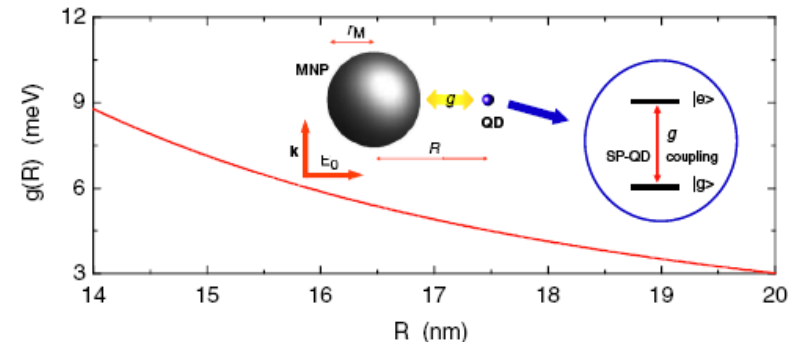
右下图：单光子产生效率



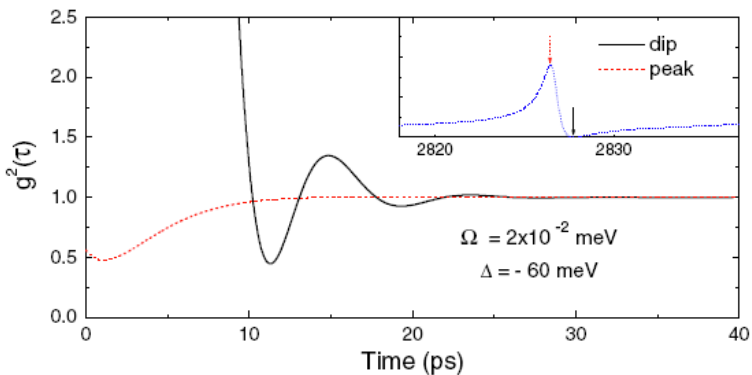
Strong coupling between quantum surface plasmons and quantum emitters



Generation of single surface plasmon source



Quantum Plasmonics with
Quantum Dot-Metal Nanoparticle
↔ Cavity QED treatment



通过SPP实现了两个qubits间的长程纠缠

$$H = \hbar\omega_0 \sum_{i=1,2} \sigma_i^\dagger \sigma_i + g_{12}(\sigma_1^\dagger \sigma_2 + \sigma_2^\dagger \sigma_1).$$

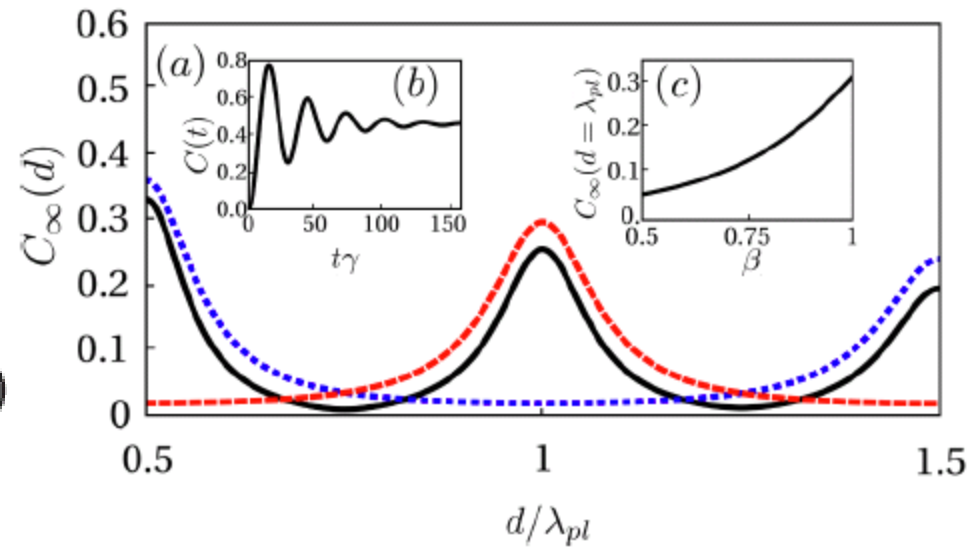
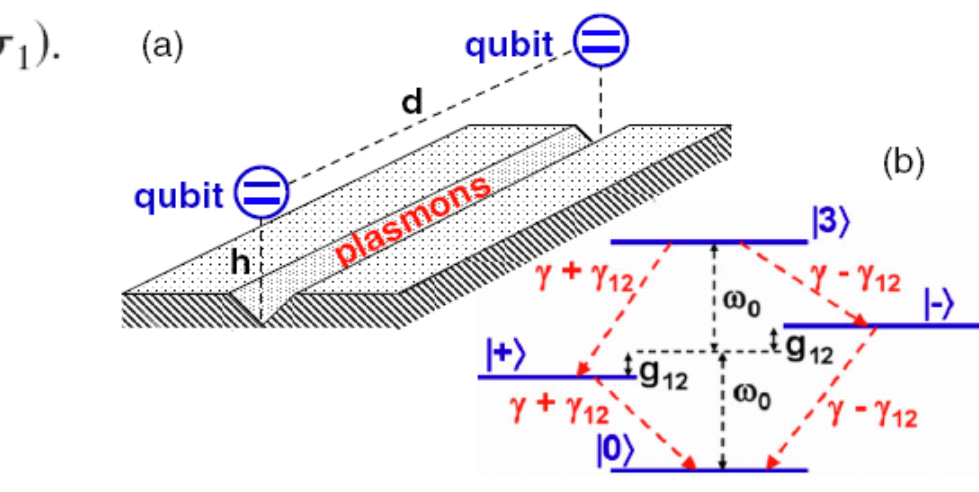
$$\begin{aligned} \partial_t \rho = & \frac{i}{\hbar} [\rho, H] + \sum_{i,j=1,2} \frac{\gamma_{ij}}{2} (2\sigma_i \rho \sigma_j^\dagger \\ & - \sigma_i^\dagger \sigma_j \rho - \rho \sigma_i^\dagger \sigma_j), \end{aligned}$$

$$g_{12} = \frac{\gamma}{2} \beta e^{-d/(2L)} \sin(k_{pl} d),$$

$$\gamma_{12} = \gamma \beta e^{-d/(2L)} \cos(k_{pl} d),$$

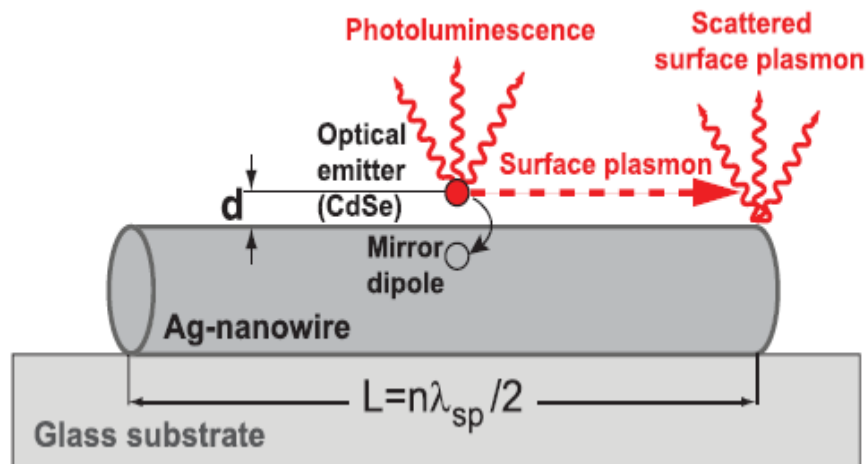
$$\{|0\rangle = |g_1, g_2\rangle, \quad |3\rangle = |e_1, e_2\rangle\},$$

$$|\pm\rangle = (1/\sqrt{2}(|e_1, g_2\rangle \pm |g_1, e_2\rangle))$$



激子-SP-光子间的转换，可做spacer

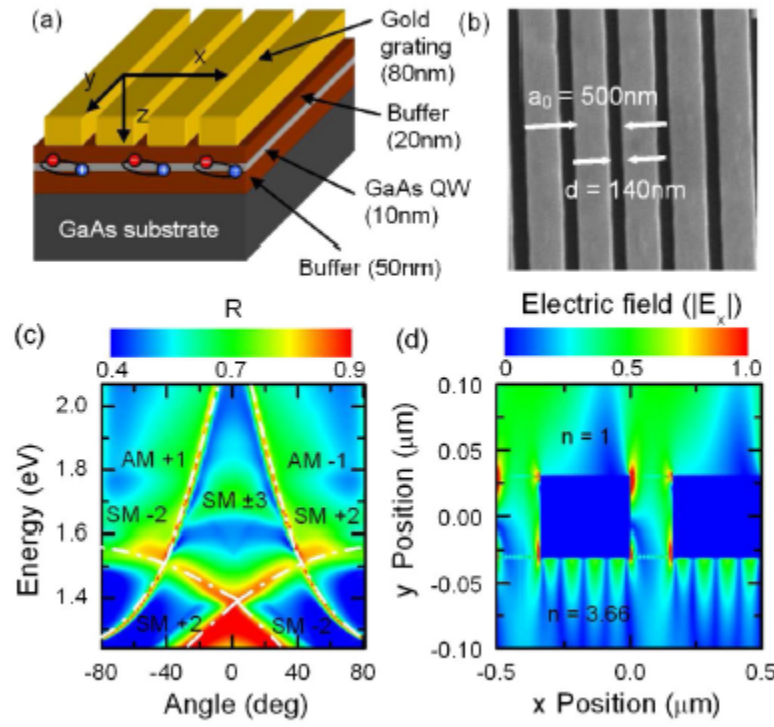
PRL 99, 136802 (2007);



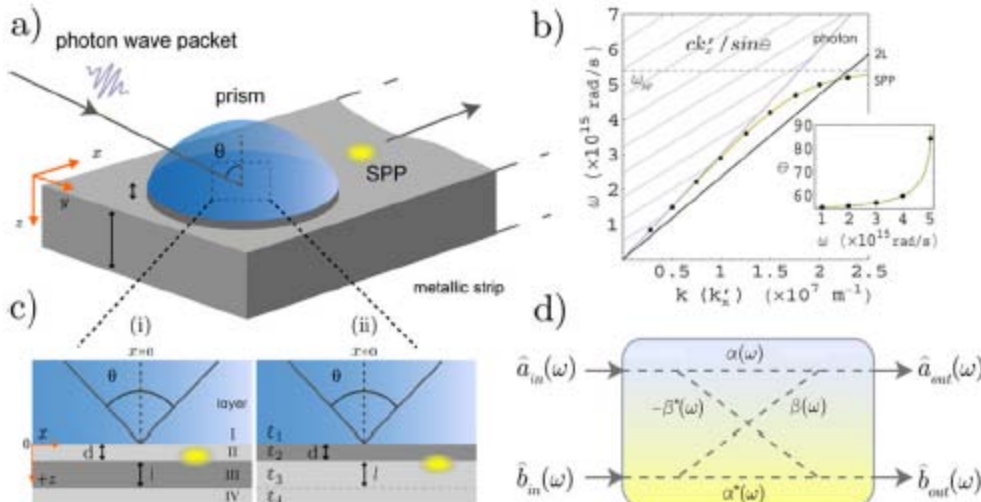
其它（仅给出示意图）

量子阱-SP间相互作用

PRL 101, 116801 (2008)



SPP的单光子激发 PRL 101, 190504 (2008)

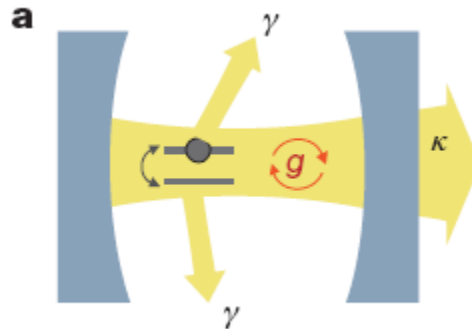


hybrid photonic architectures

The assembly of hybrid nanophotonic devices from different fundamental photonic entities—such as single molecules, nanocrystals, semiconductor quantum dots, nanowires and metal nanoparticles—can yield functionalities that exceed those of the individual subunits.

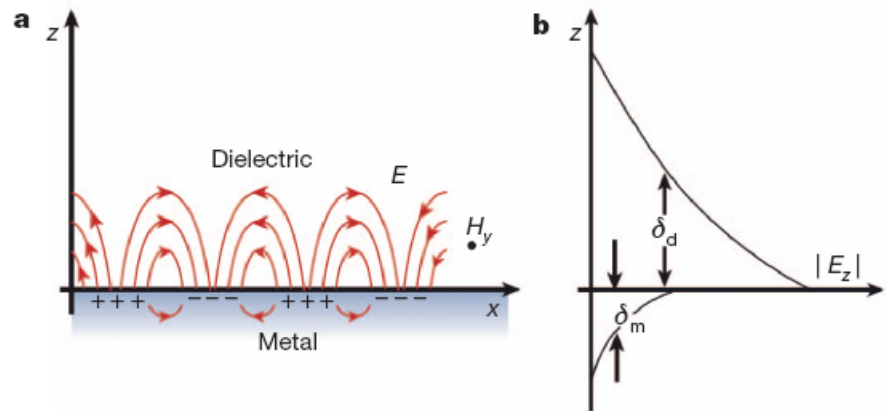
BOX 1

Cavity QED



BOX 2

Plasmonic enhancement



Functionality on the nanoscale

Light guiding and sorting

Enhanced emission and absorption

Nonlinear elements and switches

Nanophotonic–plasmonic hybrid devices

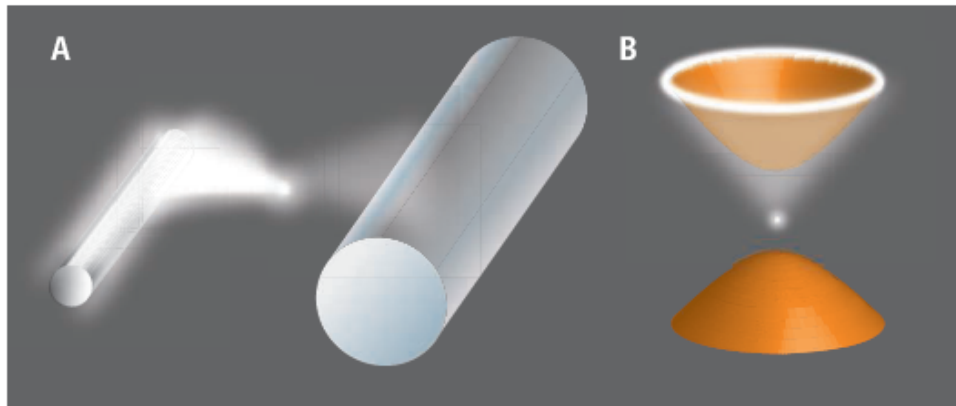
Plasmonically enhanced single-photon sources

Nanowire photonic elements

Future prospects

plasmons. Also, nonlinear interactions facilitating logical operations are feasible using CQED or plasmonic effects. There is great potential

Plasmonics Goes Quantum



Make it quantum. Building blocks of an integrated nanoscale quantum information system. (A) The nanowire supports a single plasmonic oscillation conceptually similar to a single-mode optical fiber. However, the nanoscale mode volumes of the plasmon lead to strong coupling with the quantum emitter. (B) An unorthodox approach of enhancing light-matter interaction is by tailoring the dielectric constant of a medium so that it is dielectric in one direction and metallic in another. The resulting hyperboidal dispersion relation supports infinitely many electromagnetic states for channeling light into a single-photon resonance cone.

A combined plasmonics and metamaterials approach may allow light-matter interaction to be controlled at the single-photon level.

single plasmon →
antibunching statistics
nanoscale-mode volume →
strong coupling
entangling+squeezing →
quantum information
quantum plasmonics →
Spaser
Cavity QED
QI system



5.4. 我们在交叉领域相关的几个工作

5.4.1 基于表面等离激元结构的单分子共振荧光

5.4.2 原子布居数的本征量子拍频及其在表面等离激元结构中的纳米尺度上的实现

5.4.3 表面等离激元诱导下的各向异性真空导致的亚波长尺度上的自发辐射谱线的变化

Our work: to pursue intercrossing between quantum optics and plasmonics **in weak coupling**

- 1. Resonance fluorescence in two-level system:
with one transition channel
anisotropic decay rates and near field excitation**

- 2. Quantum interferences in four-level system:
with two or more transition channel
anisotropic decay rates and near field excitation
Crossing damping under anisotropic vacuum**

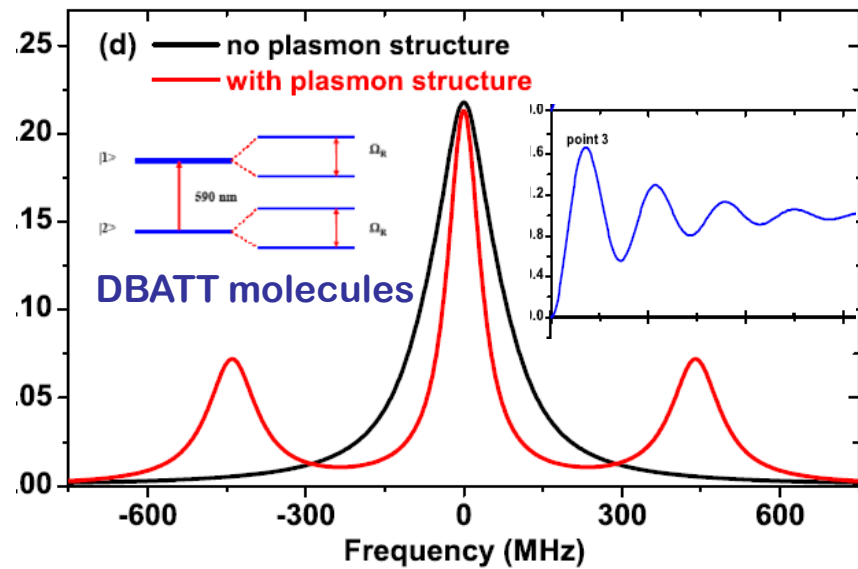
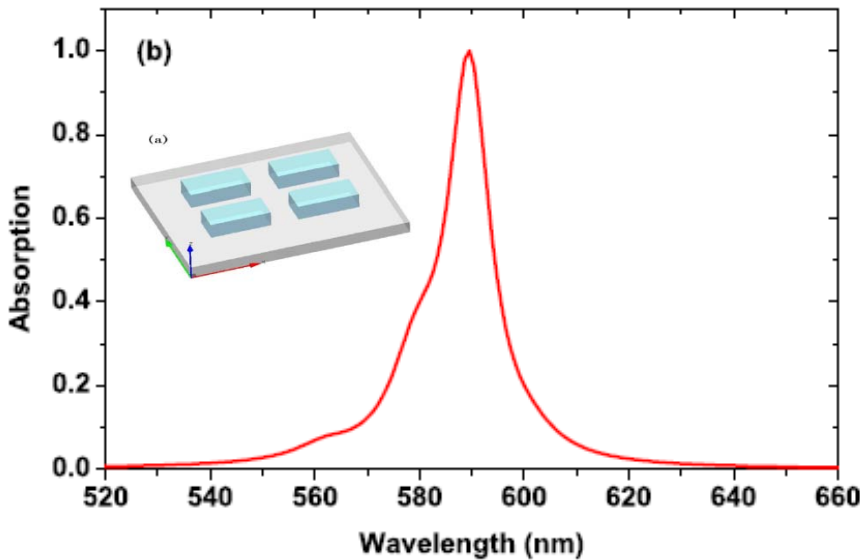
With above considerations, what would happen ?

5.4.1 Resonance fluorescence of single molecules assisted by a plasmonic structure

Basic idea

Aim to: realize resonance fluorescence of single molecules near the plasmonic structure

4 silver nanostrips, $110 \times 50 \times 40 \text{ nm}^3$



Resonance wavelength matching ($\lambda_{\text{SPR}} = \lambda_{\text{RT}} = 590 \text{ nm}$)
a balance between near field enhancement
and decay rate modification

Mollow triplet and photon antibunching

Plasmonic structure design and optimal area

The Lippmann-Schwinger equation

$$E(\mathbf{r}) = E^0(\mathbf{r}) + k^2 \int_V d\mathbf{r}' G^0(\mathbf{r}, \mathbf{r}', \omega) \epsilon_s(\mathbf{r}, \omega) \cdot E(\mathbf{r}')$$

with Green's tensor

$$G^0(\mathbf{r}, \mathbf{r}', \omega) = (\mathbf{I} - \frac{1 - ik_0 R}{k_0^2 R^2} \mathbf{I} - \frac{-3 + 3ik_0 R + k_0^2 R^2}{k_0^2 R^4} \mathbf{R} \mathbf{R}) \frac{\exp[ik_0 R]}{4\pi R}$$

in the arbitrarily shaped nanostructures

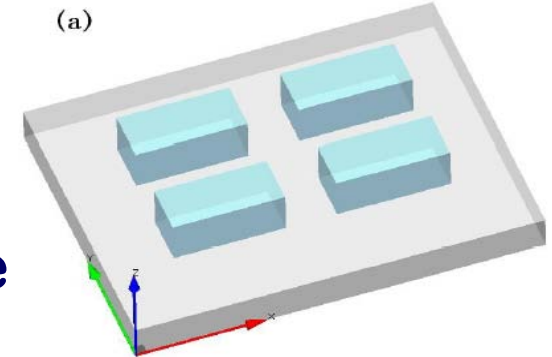
Green's tensor method:

solving the optical near field

Green's matrix method:

designing surface plasmon resonance

by solving the eigensystems



A unique design of silver four-nanostrip system
with surface plasmon resonance at $\lambda=590\text{nm}$

Optimal coefficient

$$R_\alpha = \frac{E_\alpha/E_0}{\Gamma_{\alpha\alpha}/\Gamma_0}$$

$\Gamma_{\alpha\alpha}/\Gamma_0 = 3\lambda \operatorname{Im}(G_{\alpha\alpha})$ where $G_{\alpha\alpha}$ is the Green's tensor

formulas for resonance fluorescence of two-level system:

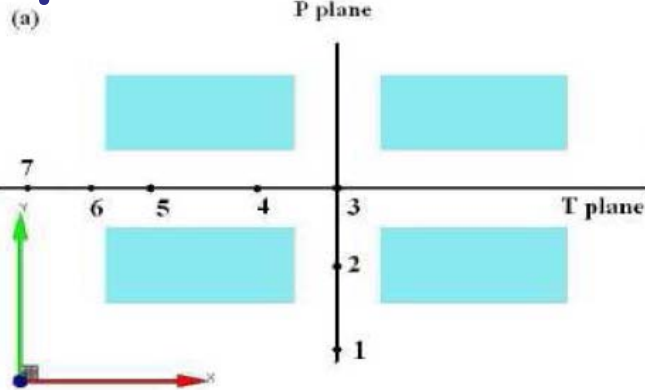
$$S(\vec{r}, \omega) = \frac{I_0(\vec{r})}{8\pi} \left[\frac{3\Gamma/4}{(\omega - \Omega_R - \omega_0)^2 + (3\Gamma/4)^2} + \frac{\Gamma}{(\omega - \omega_0)^2 + (\Gamma/2)^2} + \frac{3\Gamma/4}{(\omega + \Omega_R - \omega_0)^2 + (3\Gamma/4)^2} \right]$$

--

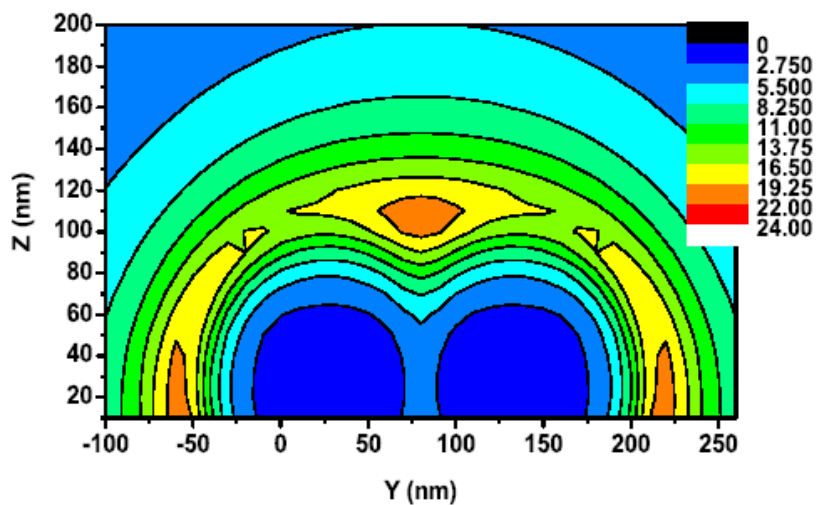
$$g^{(2)}(\tau) = 1 - (\cos \mu\tau + \frac{3\Gamma}{4\mu} \sin \mu\tau) e^{-3\Gamma\tau/4} \text{ with } \mu = (\Omega_R^2 - (\Gamma/4)^2)^{1/2}$$

**Using the optimal coefficient, to find specific regions where a large near field enhancement and a small modification of decay rate simultaneously exist.
Mollow triplet and photons antibunching.**

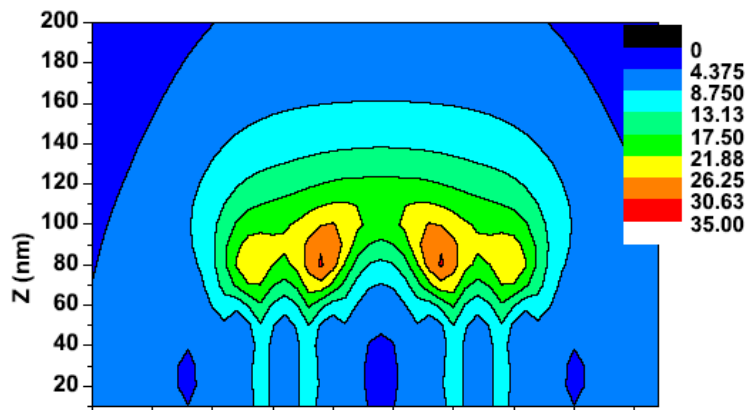
Optimal nanoarea



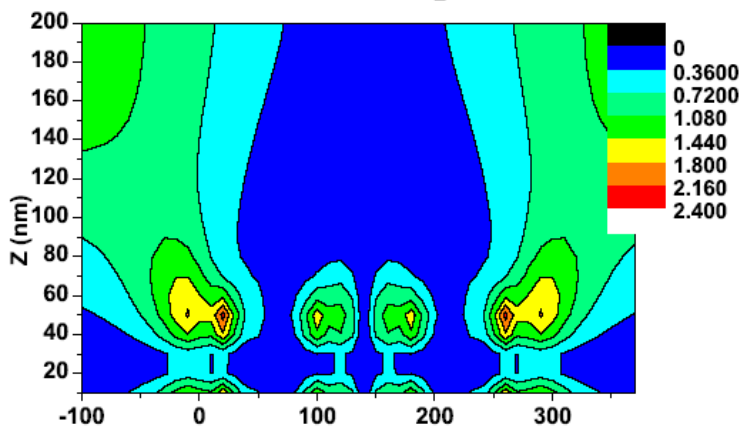
(b) Optimal coefficient R_x of P plane



(c) Optimal coefficient R_x of T plane

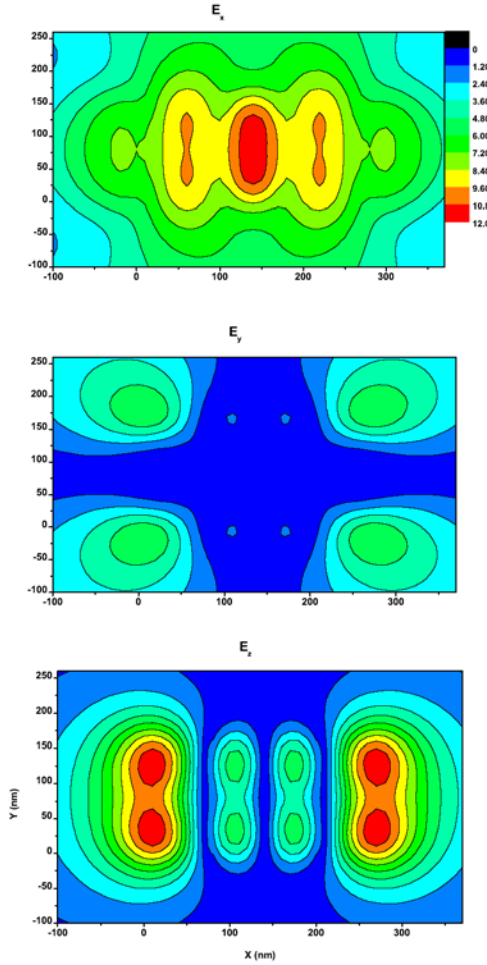


Optimal coefficient R_z of T plane

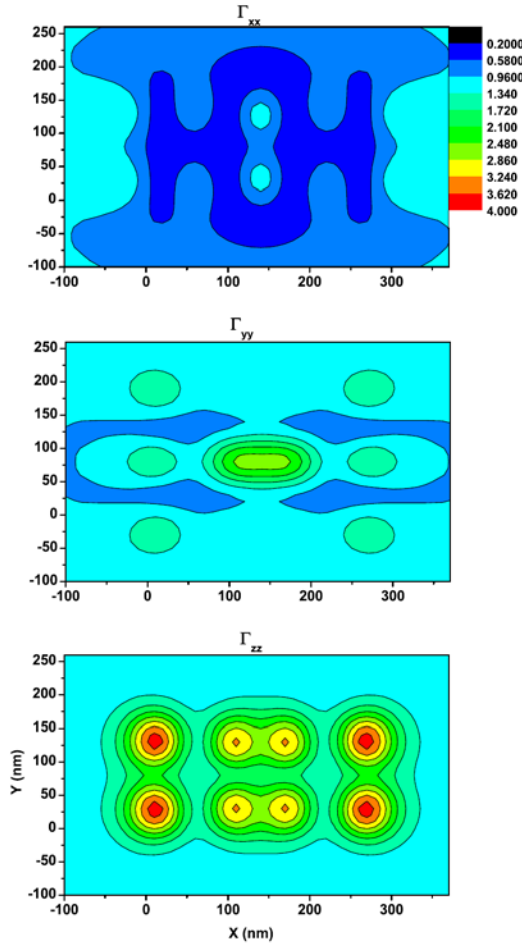


Specific regions 30 to 100 nm away from the metal surface, where R_x reaches 10~30.

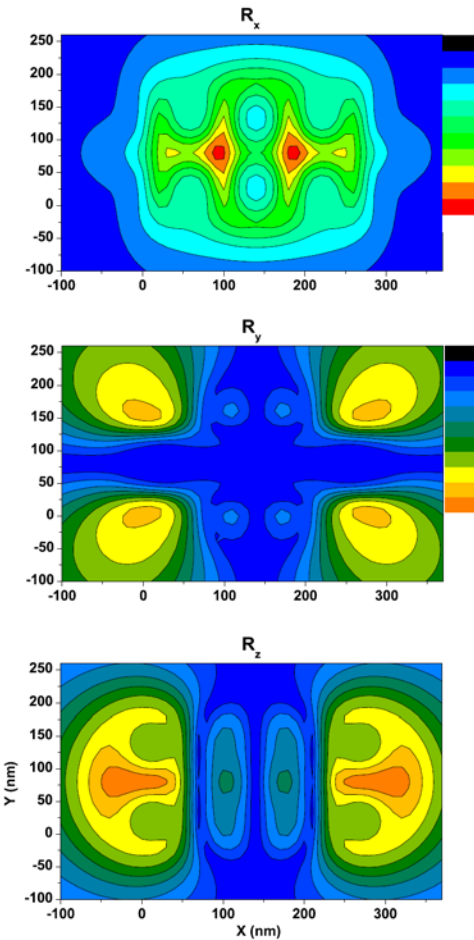
(a) Electric fields



(b) Decay rates



(c) Optimal coefficients

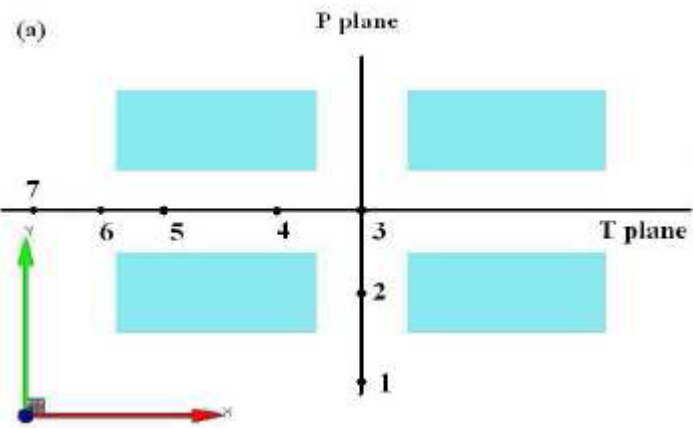


In xy plane 50nm away from metal surface above gaps

We find: $R_x = 10 \sim 30$ whereas $R_y < 5$ and $R_z < 5$

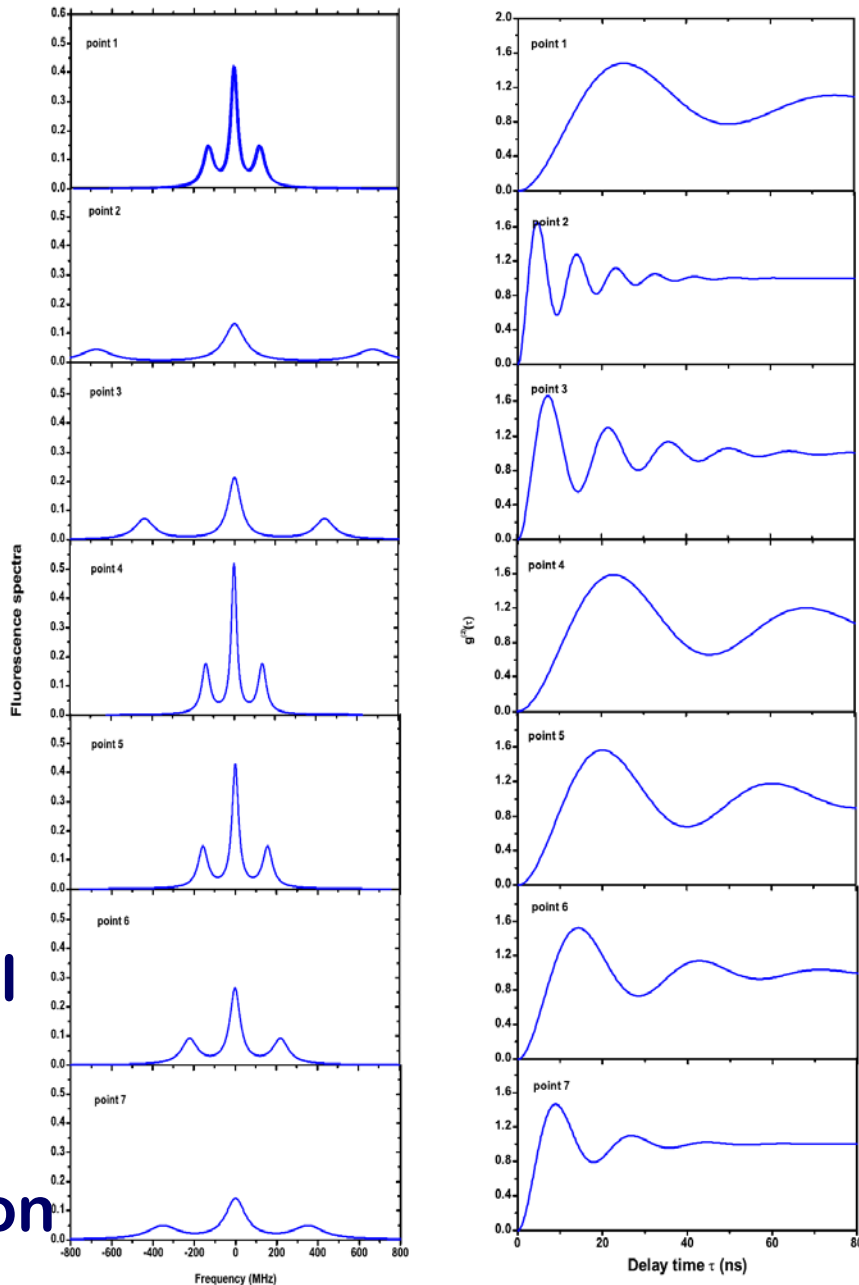
A good directivity of emission

Resonance fluorescence



xy plane 50nm away from surface

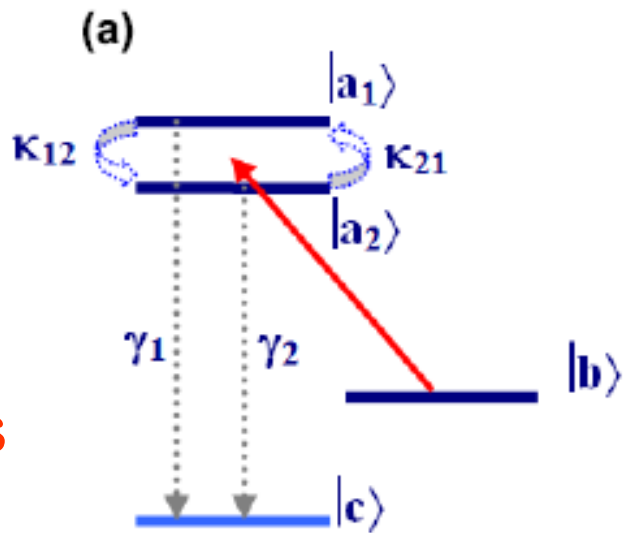
1. Mollow triplet and photon antibunching in fluorescence.
2. Narrower spectra than natural linewidth due to cavity effects
3. sideband and linewidth of spectra sensitive to the location



5.4.2 Intrinsic Quantum Beats of Atomic Populations in Isotropic and Plasmon-induced anisotropic vacuum

Model setup

Schrödinger equation
in isotropic vacuum and
W-W approximations
with crossing damping terms



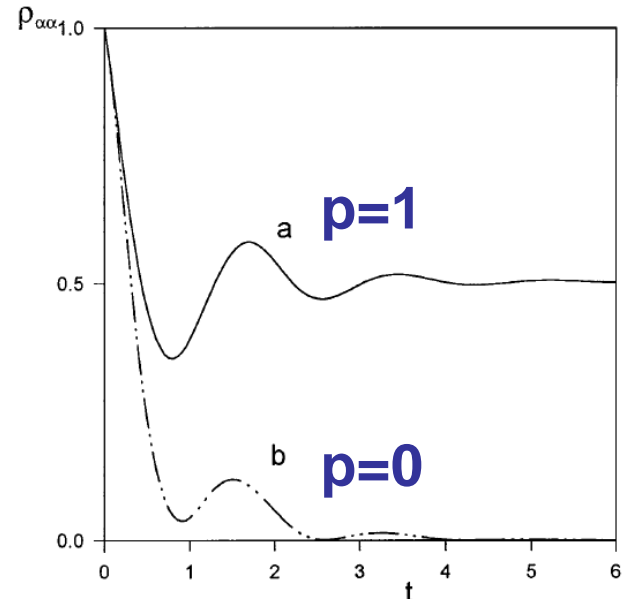
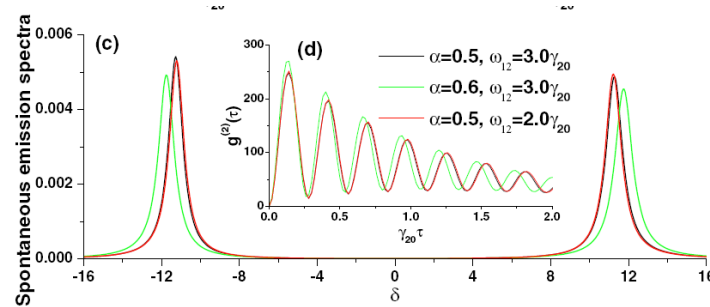
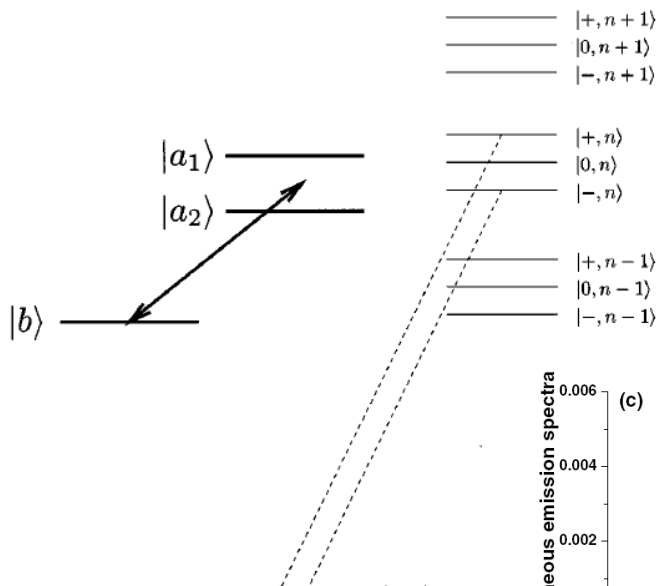
$$\begin{aligned}
 \frac{d}{dt} A^{(1)}(t) &= -\frac{\gamma_1}{2} A^{(1)}(t) - p \frac{\sqrt{\gamma_1 \gamma_2}}{2} A^{(2)}(t) e^{i\omega_{12} t} + \Omega_1 e^{i\Delta_1 t} B(t), \\
 \frac{d}{dt} A^{(2)}(t) &= -\frac{\gamma_2}{2} A^{(2)}(t) - p \frac{\sqrt{\gamma_1 \gamma_2}}{2} A^{(1)}(t) e^{-i\omega_{12} t} + \Omega_2 e^{i\Delta_2 t} B(t), \\
 \frac{d}{dt} B(t) &= -\Omega_1^* e^{-i\Delta_1 t} A^{(1)}(t) - \Omega_2^* e^{-i\Delta_2 t} A^{(2)}(t), \\
 \frac{d}{dt} C_k(t) &= -g_1^* A^{(1)}(t) e^{-i(\omega_{a1c} - \omega_k)t} - g_2^* A^{(2)}(t) e^{-i(\omega_{a2c} - \omega_k)t}.
 \end{aligned}$$

Population trapping condition

The populations are trapped in upper levels due to quantum interferences.

$$\Delta_1 |\Omega_2|^2 + \Delta_2 |\Omega_1|^2 = 0,$$

$$P \frac{\Omega_1}{\Omega_2} = \sqrt{\frac{\gamma_1}{\gamma_2}} \quad (p = \pm 1).$$



Dressed state analysis

The spontaneous emission from $|0,n\rangle$ to $|c\rangle$ is zero →
Spontaneous emission cancellation

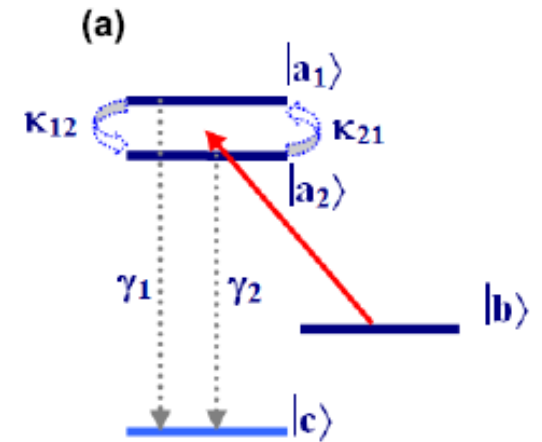
In anisotropic vacuum and W-W approximations

$$\frac{d}{dt} A^{(1)}(t) = -\frac{\gamma_1}{2} A^{(1)}(t) - \frac{\kappa_2}{2} A^{(2)}(t) e^{i\omega_{12}t} + \Omega_1 e^{i\Delta_1 t} B(t),$$

$$\frac{d}{dt} A^{(2)}(t) = -\frac{\gamma_2}{2} A^{(2)}(t) - \frac{\kappa_1}{2} A^{(1)}(t) e^{-i\omega_{12}t} + \Omega_2 e^{i\Delta_2 t} B(t),$$

$$\frac{d}{dt} B(t) = -\Omega_1^* e^{-i\Delta_1 t} A^{(1)}(t) - \Omega_2^* e^{-i\Delta_2 t} A^{(2)}(t),$$

$$\frac{d}{dt} C_k(t) = -g_1^* A^{(1)}(t) e^{-i(\omega_{a1c} - \omega_k)t} - g_2^* A^{(2)}(t) e^{-i(\omega_{a2c} - \omega_k)t}.$$



decay rates and crossing damping in terms of Green's tensor.

$$\gamma_{1,2} = \Gamma_{xx} \cos^2 \theta_{1,2} + \Gamma_{zz} \sin^2 \theta_{1,2} \quad \Gamma_{zz}/\gamma_0 = 3\lambda_{ac} \text{Im}G_{zz}$$

$$\kappa = \Gamma_{xx} \cos \theta_1 \cos \theta_2 + \Gamma_{zz} \sin \theta_1 \sin \theta_2 \quad \Gamma_{xx}/\gamma_0 = 3\lambda_{ac} \text{Im}G_{xx}$$

new trapping conditions $\gamma_1 |\Omega_2|^2 + \gamma_2 |\Omega_1|^2 - \kappa (\Omega_1 \Omega_2^* + \Omega_2 \Omega_1^*) = 0,$

“Two parallel dipoles” can’t be broken $\Delta_1 |\Omega_2|^2 + \Delta_2 |\Omega_1|^2 = 0.$

Quantum beats of population oscillations

Skip the complex formulas

Beat frequency:

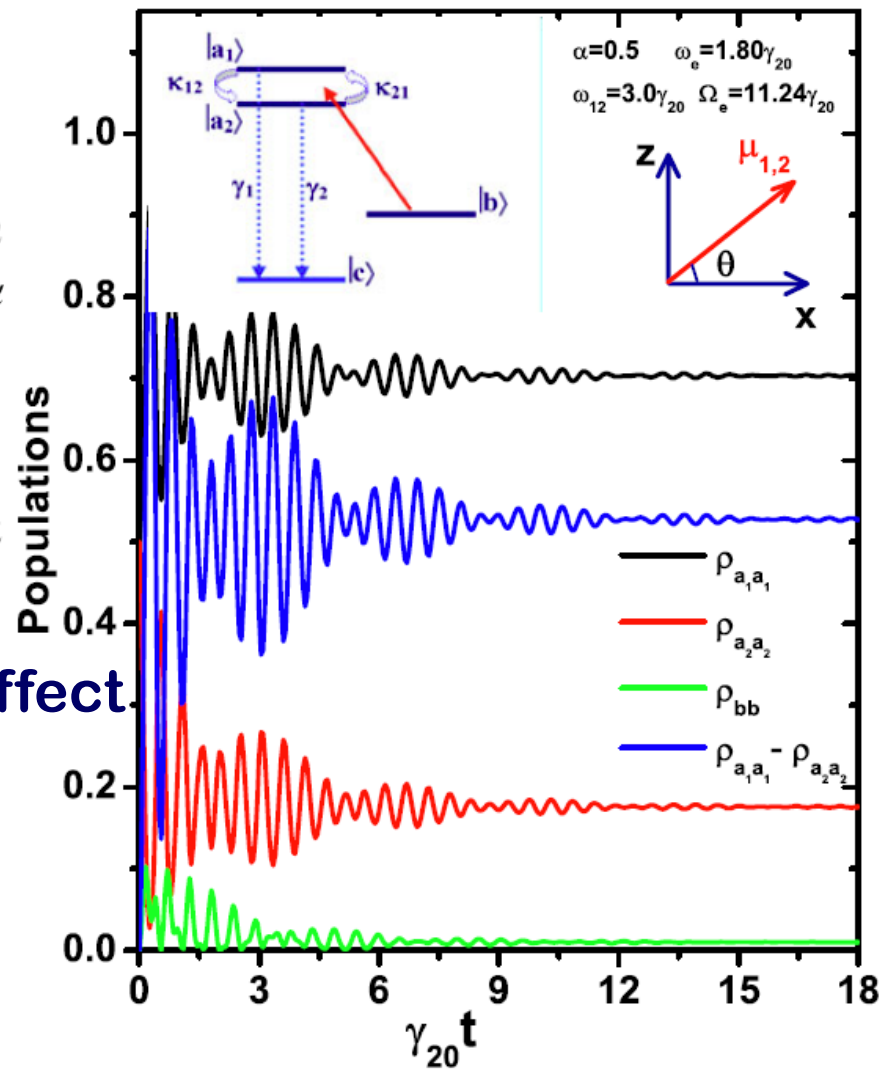
$$\omega_e = \frac{1-\alpha^2}{1+\alpha^2} \omega_{12}$$

$$\begin{aligned}\omega_{a_1} - \omega_{a_2} &= \omega_{12} \\ |\vec{\mu}_1| / |\vec{\mu}_2| &= \alpha\end{aligned}$$

Rabi frequency:

$$|\Omega_e|^2 = \left[\frac{\alpha}{1+\alpha^2} \omega_{12} \right]^2 + |\Omega_1|^2 + |\Omega_2|^2$$

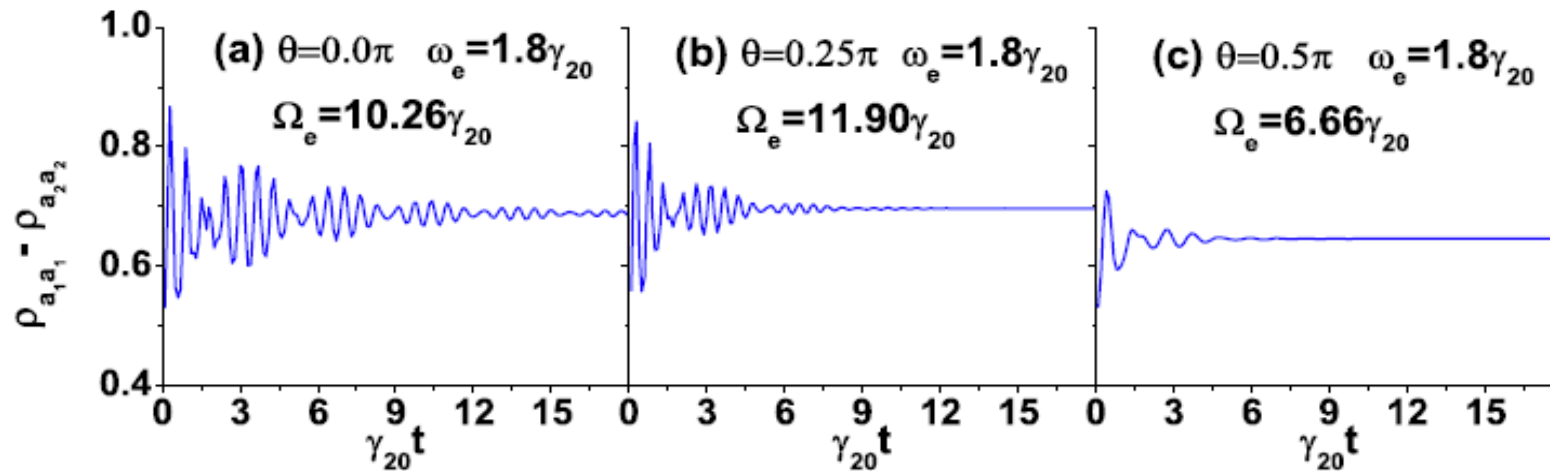
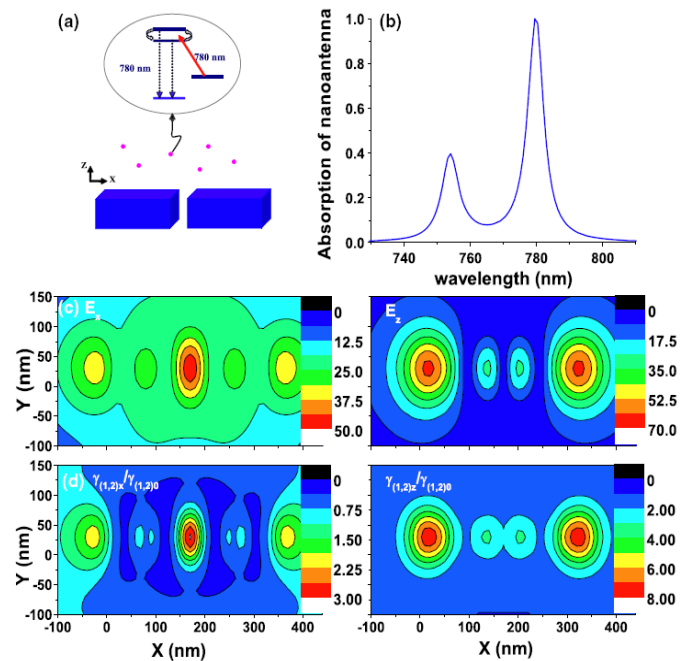
New quantum interference effect in isotropic and anisotropic vacuum. Beat frequency is determined by spacing and dipole moment ratio.



Nanoscale Realization in Plasmon-Induced anisotropic vacuum

Right: absorption, near field distribution, and decay rates of silver nanoantenna at resonant wavelength of 780 nm.

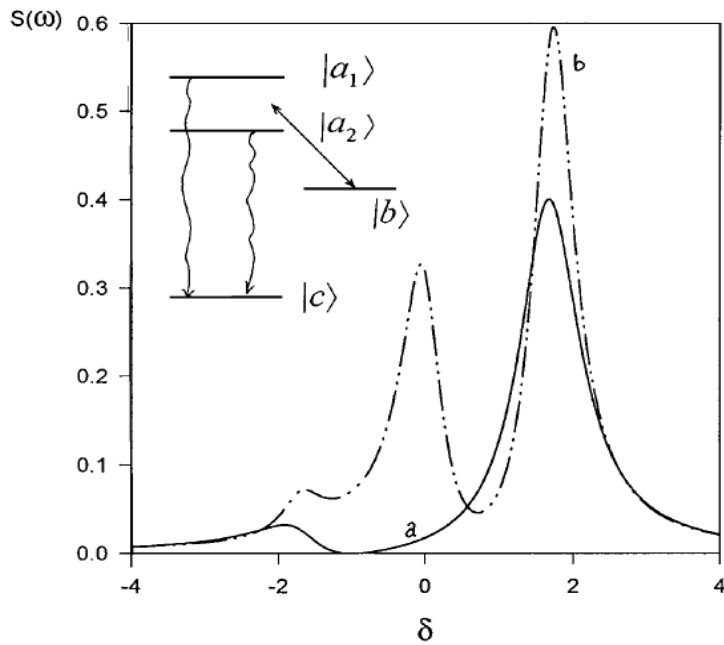
Bottom: quantum beats of atomic populations in near field region



5.4.3 Surface-Plasmon-Induced Modification on the Spontaneous Emission Spectrum via Subwavelength-Confining Anisotropic Purcell factor

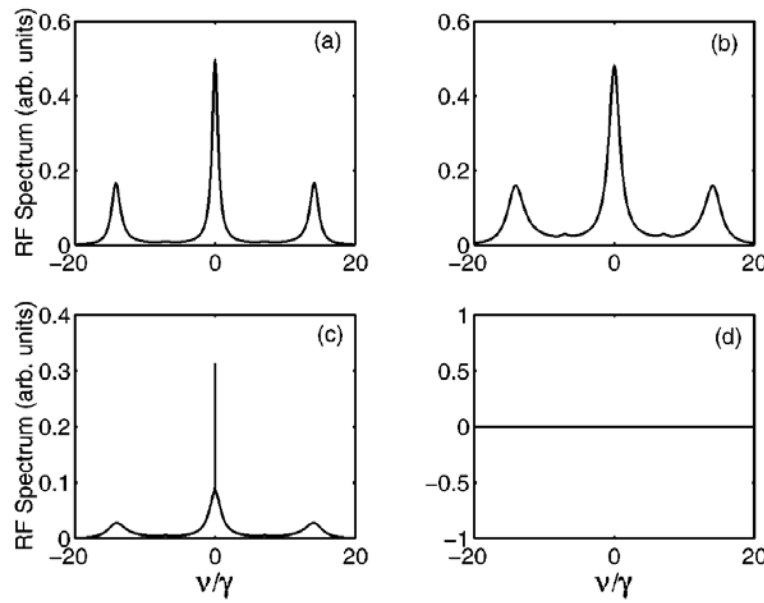
Quantum interferences In a vacuum

crossing damping between two closely lying upper states



- a: parallel dipole moments
spontaneous emission cancellation
b: orthogonal dipole moments
three emission peaks

For nearly parallel dipoles,
ultranarrow spectral lines as
crossing damping increases



Theory

Green's tensor coefficients

$$\Gamma_{zz}/\gamma_0 = 3\lambda_{ac} \text{Im}G_{zz}, \quad \Gamma_{xx}/\gamma_0 = 3\lambda_{ac} \text{Im}G_{xx}$$

decay rates and crossing damping in anisotropic vacuum

$$\gamma_{1,2} = \Gamma_{xx} \cos^2 \theta_{1,2} + \Gamma_{zz} \sin^2 \theta_{1,2}$$

$$\kappa = \Gamma_{xx} \cos \theta_1 \cos \theta_2 + \Gamma_{zz} \sin \theta_1 \sin \theta_2$$

Master equation, dressed state analysis

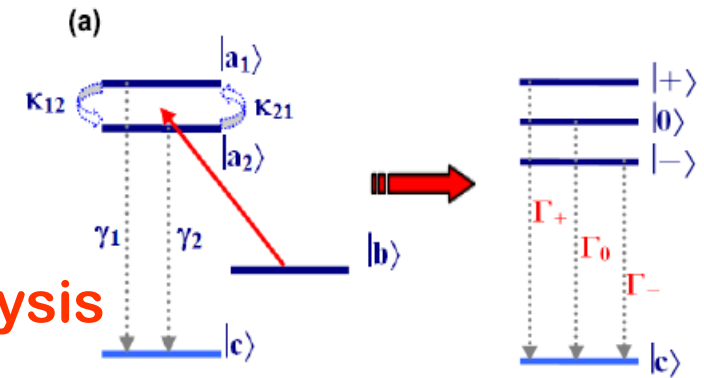
quantum regression theorem

linewidths of the central peak and sidebands

$$\Gamma_0 = (\gamma_1 + \gamma_2 - 2\kappa)4\eta^2,$$

$$\Gamma_{\pm} = (\gamma_1 + \gamma_2) \frac{1 + \epsilon^2}{4} \pm (\gamma_1 - \gamma_2) \frac{\epsilon}{2} + \kappa \frac{1 - \epsilon^2}{2}$$

$$\epsilon = \omega_{12}/\Omega_R, \quad \eta = \Omega/\Omega_R$$



$$\begin{aligned}\Gamma_0 &\doteq (\gamma_1 + \gamma_2)/2 - \kappa \\ \Gamma_{\pm} &\doteq (\gamma_1 + \gamma_2)/4 + \kappa/2\end{aligned}$$

Mechanism of linewidth control

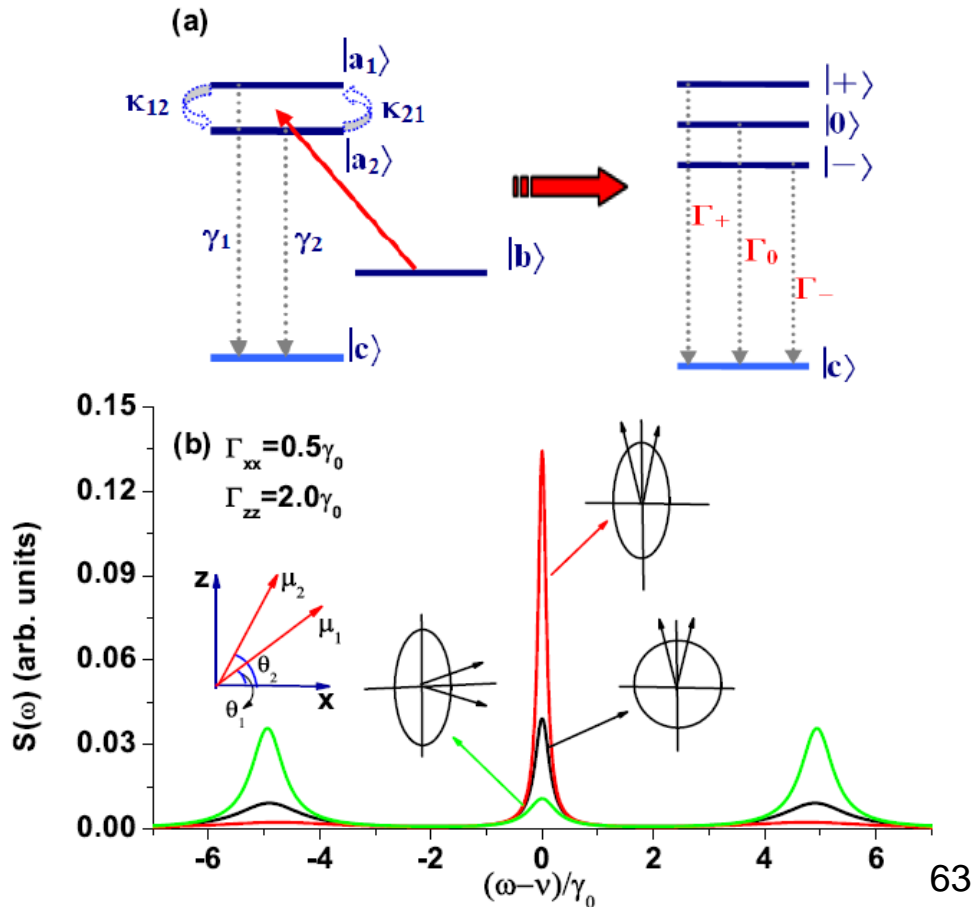
If the polarization angle bisector of two dipole moments lies along the major/minor axis of the effective decay rate ellipse, destructive/constructive interference narrows/widens the center spectral lines associated with fluorescence.

Enlarging the anisotropy increases the variation.

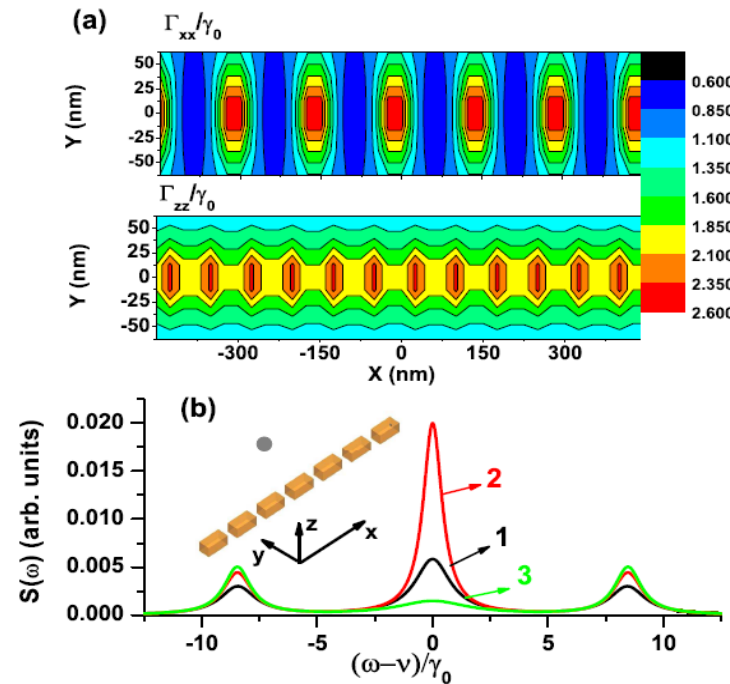
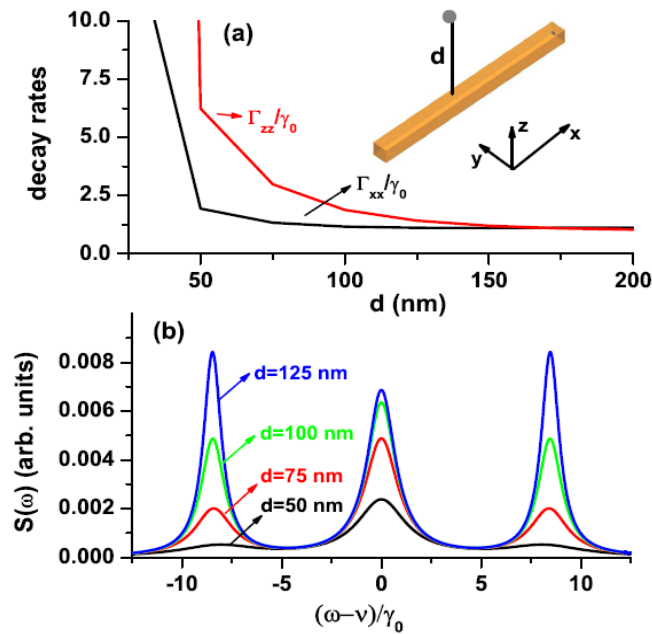
$$\Gamma_0/\Gamma_{\pm} = 0.0528$$

$$\Gamma_0/\Gamma_{\pm} = 0.2112$$

$$\Gamma_0/\Gamma_{\pm} = 0.8446$$

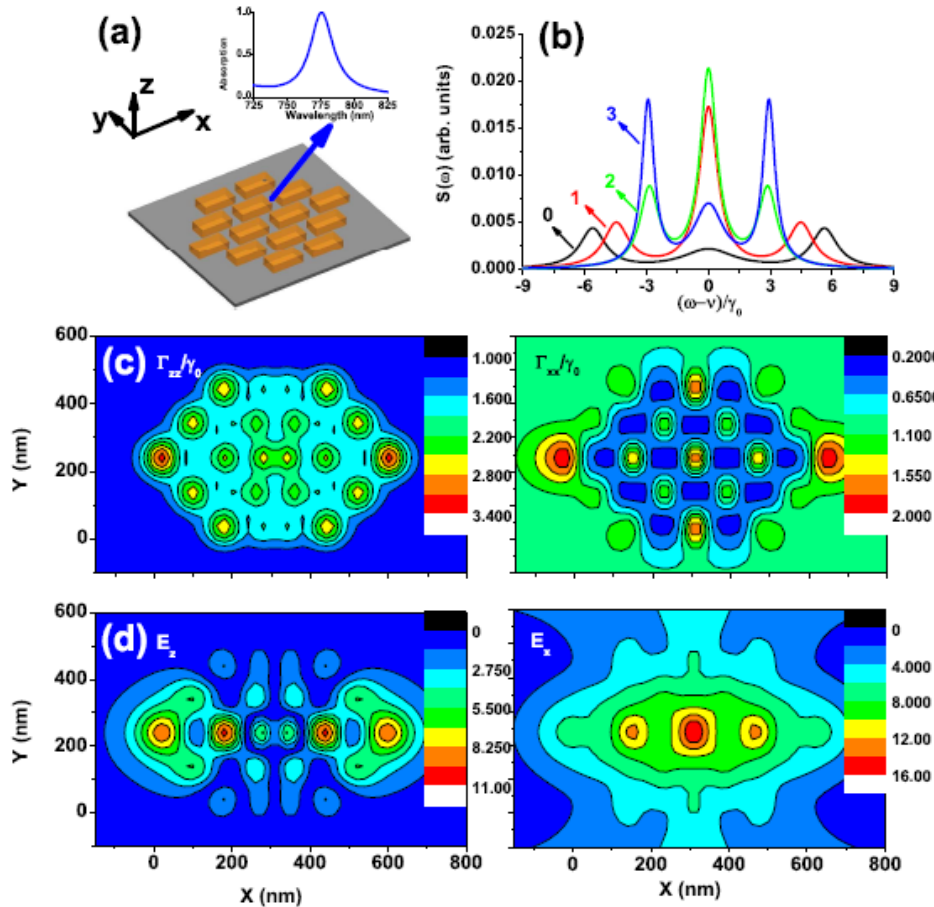


In the Surface-Plasmon-Induced Subwavelength-Confinement Anisotropic Purcell factor



Left: Rapid spectral line narrowing of atom approaching a metallic nanowire

Right: the linewidth “pulsing” following periodically-varying decay rates near a periodic metallic nanostructure



Top: dramatic modification on the spontaneous emission spectrum near a custom-designed resonant plasmon nanostructure, even subnatural linewidth

Summary

- 1. Mollow triplet and photon antibunching of molecular fluorescence assisted by plasmonic structure**
- 2. Quantum beats of atomic populations in isotropic vacuum, its nanoscale realization in plasmon-induced anisotropic vacuum**
- 3. Mechanism of spontaneous emission spectrum control, its proof and demonstration in subwavelength-confined anisotropic vacuum**

Next, strong coupling

Significance:

1. bridges the fields of quantum optics and plasmonics
2. low-level light nonlinear optical properties
3. efficient coupling of single photons into the single plasmons.
4. Superior to the cavity QED, anisotropic vacuum and plasmon excitation cover a broad frequency region and require no sophisticated experimental setups to achieve the resonances.
5. for applications in ultracompact active quantum devices.

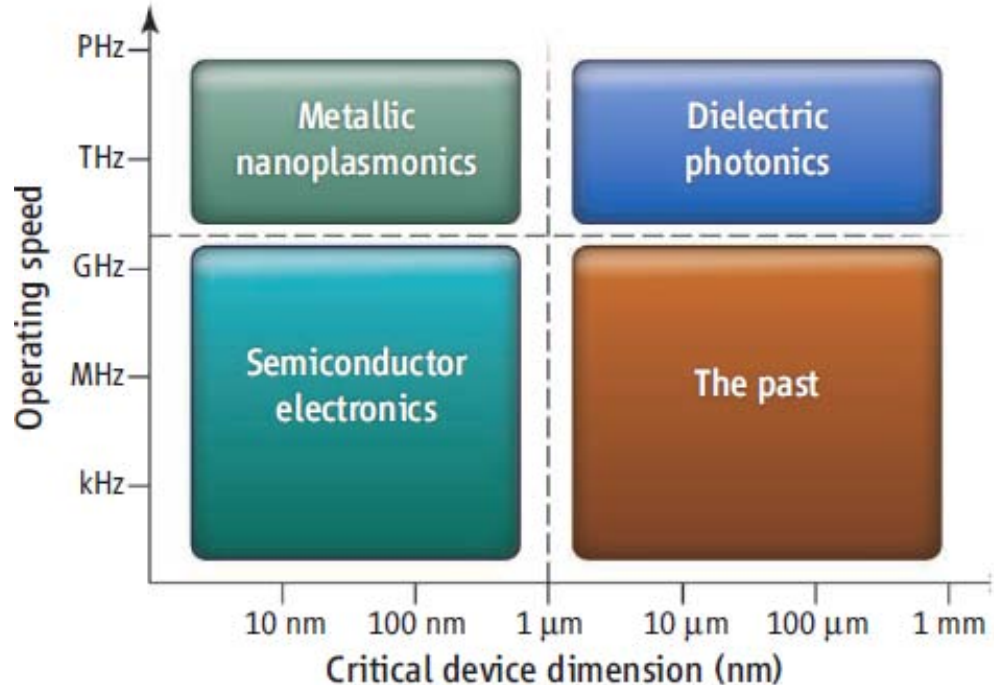
Experiments !

本章结束语：

目前，表面等离激元和量子体系的交叉研究还处于起始阶段，还有很多问题研究得并不多，如 **SPP** 的量子化，量子相干性，**SPP** 做为一个量子如何与多能级的原子分子相互作用，以及 **SPP** 如何用于量子信息过程的研究等。

Plasmonics

结束语

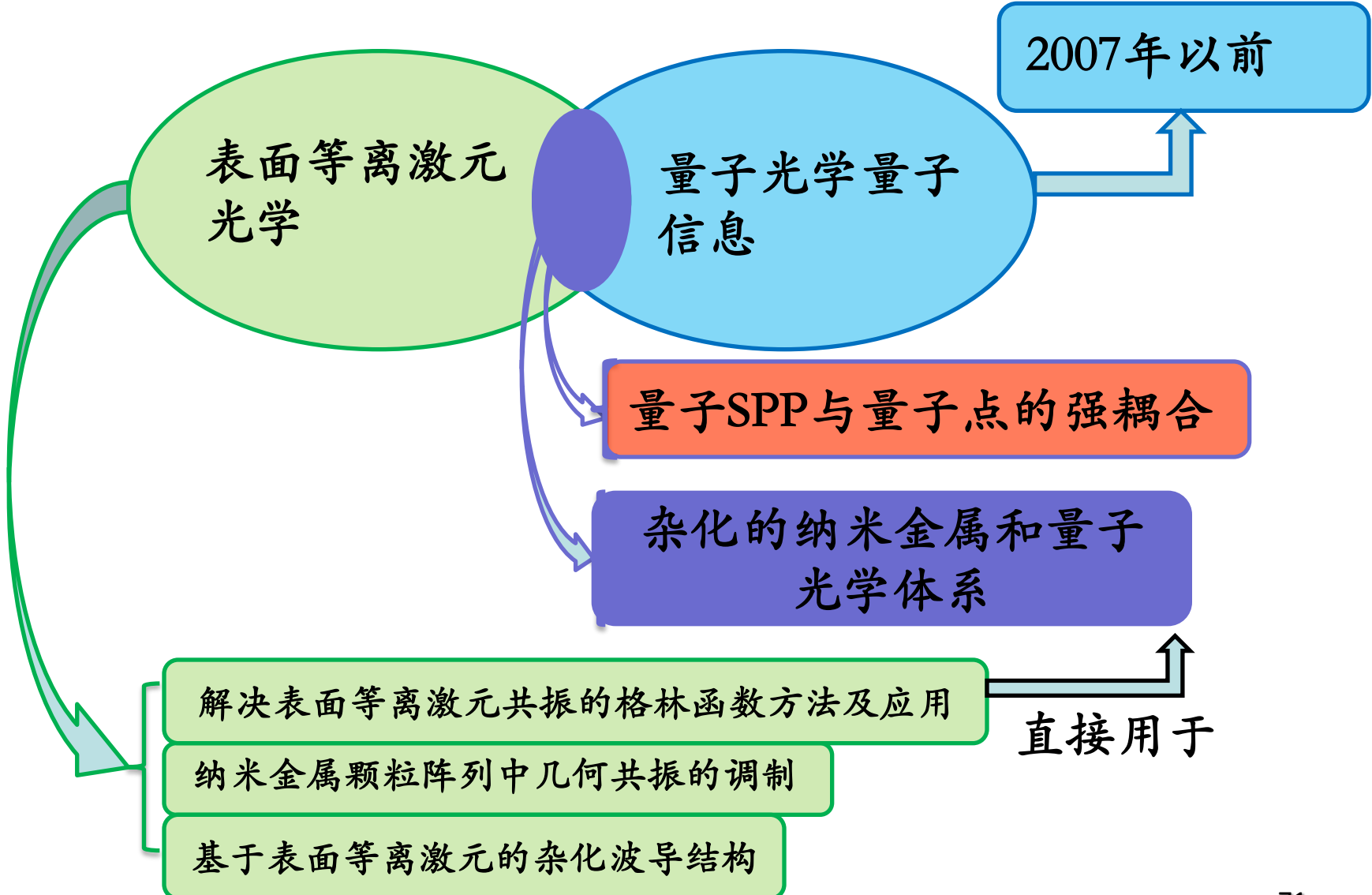


表面等离激元光学是纳米尺度上光子学和电子学的结合，在光子回路，数据存储，光谱学，生物光子学，太阳能，非线性光学，量子光学和量子信息方面都有应用，能够实现纳米尺度上控制光的超小器件。

未来发展方向

come. Important new directions for this field include the following: (1) merging plasmonics with quantum systems,^{74,79} providing challenges for both theory and experiment; (2) coherent phenomena in plasmonics, where Fano resonances, superradiance, and plasmon-induced transparency result in novel new lineshapes and plasmonic properties;^{107,21} (3) active plasmonic devices and media; new types of devices and media combining plasmonics with other functional materials for active and nonlinear responses;¹⁰⁰ (4) improved sensors and detectors; from ultrasmall detectors to LSPR sensors with single molecule sensitivity and specificity,⁵¹ there are many possibilities for advancing the ability to increase detection sensitivities and responsivities; (5) the role of plasmons in modifying chemical reactions; and (6) biomedical applications, where new types of nanoscale devices can be developed for diagnosis¹¹ and treatment of diseases, to improve treatment efficacy, and to develop prevention strategies for global health challenges. We predict the fu-

我们小组的工作





附录： 分子荧光(molecular fluorescence, MF)的知识

Luminescence (发光) : an emission of ultraviolet, visible or infrared photons from an electronically excited species, including fluorescence(荧光) and phosphorescence(磷光)

MF 的作用： 是一种很好的分析各种类的成份的工具；还可分析各种活体生物结构和动力学过程；还可以做高灵敏度的传感器。

MF 的发展简史：

1565	N. Monardes	Emission of light by an infusion of wood Lignum Nephriticum (first reported observation of fluorescence)
1602	V. Cascariolo	Emission of light by Bolognese stone (first reported observation of phosphorescence)
1640	Licetus	Study of Bolognese stone. First definition as a non-thermal light emission
1833	D. Brewster	Emission of light by chlorophyll solutions and fluorspar crystals
1845	J. Herschel	Emission of light by quinine sulfate solutions (epipolar dispersion)
1842	E. Becquerel	Emission of light by calcium sulfide upon excitation in the UV. First statement that the emitted light is of longer wavelength than the incident light
1852	G. G. Stokes	Emission of light by quinine sulfate solutions upon excitation in the UV (refrangibility of light)
1853	G. G. Stokes	Introduction of the term fluorescence
1858	E. Becquerel	First phosphoroscope
1867	F. Goppelsröder	First fluorometric analysis (determination of Al(III) by the fluorescence of its morin chelate)
1871	A. Von Baeyer	Synthesis of fluorescein
1888	E. Wiedemann	Introduction of the term luminescence

1905,	E. L. Nichols and	First fluorescence excitation spectrum of a dye
1910	E. Merrit	
1907	E. L. Nichols and E. Merrit	Mirror symmetry between absorption and fluorescence spectra
1918	J. Perrin	Photochemical theory of dye fluorescence
1919	Stern and Volmer	Relation for fluorescence quenching
1920	F. Weigert	Discovery of the polarization of the fluorescence emitted by dye solutions
1922	S. J. Vavilov	Excitation-wavelength independence of the fluorescence quantum yield
1923	S. J. Vavilov and W. L. Levshin	First study of the fluorescence polarization of dye solutions
1924	S. J. Vavilov	First determination of fluorescence yield of dye solutions
1924	F. Perrin	Quantitative description of static quenching (active sphere model)
1924	F. Perrin	First observation of alpha phosphorescence (E-type delayed fluorescence)
1925	F. Perrin	Theory of fluorescence polarization (influence of viscosity)
1925	W. L. Levshin	Theory of polarized fluorescence and phosphorescence
1925	J. Perrin	Introduction of the term delayed fluorescence Prediction of long-range energy transfer

1926	E. Gaviola	First direct measurement of nanosecond lifetimes by phase fluorometry (instrument built in Pringsheim's laboratory)
1926	F. Perrin	Theory of fluorescence polarization (sphere). Perrin's equation Indirect determination of lifetimes in solution. Comparison with radiative lifetimes
1927	E. Gaviola and P. Pringsheim	Demonstration of resonance energy transfer in solutions
1928	E. Jette and W. West	First photoelectric fluorometer
1929	F. Perrin	Discussion on Jean Perrin's diagram for the explanation of the delayed fluorescence by the intermediate passage through a metastable state First qualitative theory of fluorescence depolarization by resonance energy transfer
1929	J. Perrin and Choucroun	Sensitized dye fluorescence due to energy transfer
1932	F. Perrin	Quantum mechanical theory of long-range energy transfer between atoms
1934	F. Perrin	Theory of fluorescence polarization (ellipsoid)
1935	A. Jablonski	Jablonski's diagram
1944	Lewis and Kasha	Triplet state
1948	Th. Förster	Quantum mechanical theory of dipole-dipole energy transfer

分子能级示意图

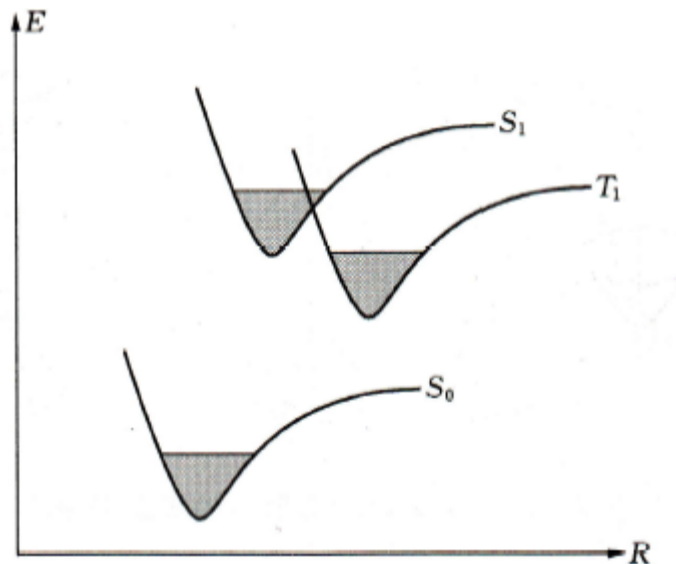


图 2.1.3 常见的单重态和三重态势能相对位置

可以看到：分子能级通常有单态和三重态，它们之间有如上图所示的相对位置。由于分子有较多的振动能级，相对于原子来说，能级间距较小（如图中阴影部分），这也是分子光谱较宽的原因。

Franck-Condon原理

跃迁前:分子处于基态的最低能态 $\nu=0$

跃迁时:分子垂直跃迁到上方的激发态,而 $E(\Psi_\alpha)$ 和 $E(\Psi_0)$ 存在红移

跃迁后: $\langle \Psi_0 | \Psi_\alpha \rangle^2$ 最大时对应光谱中的最高峰。

FC原理:原子和原子团的直径 1nm 以内,光波通过原子团的时间 $10^{-17}s$,而分子键的振动周期是 $10^{-14}s$;基本上认为,跃迁的瞬间分子构型保持不变。

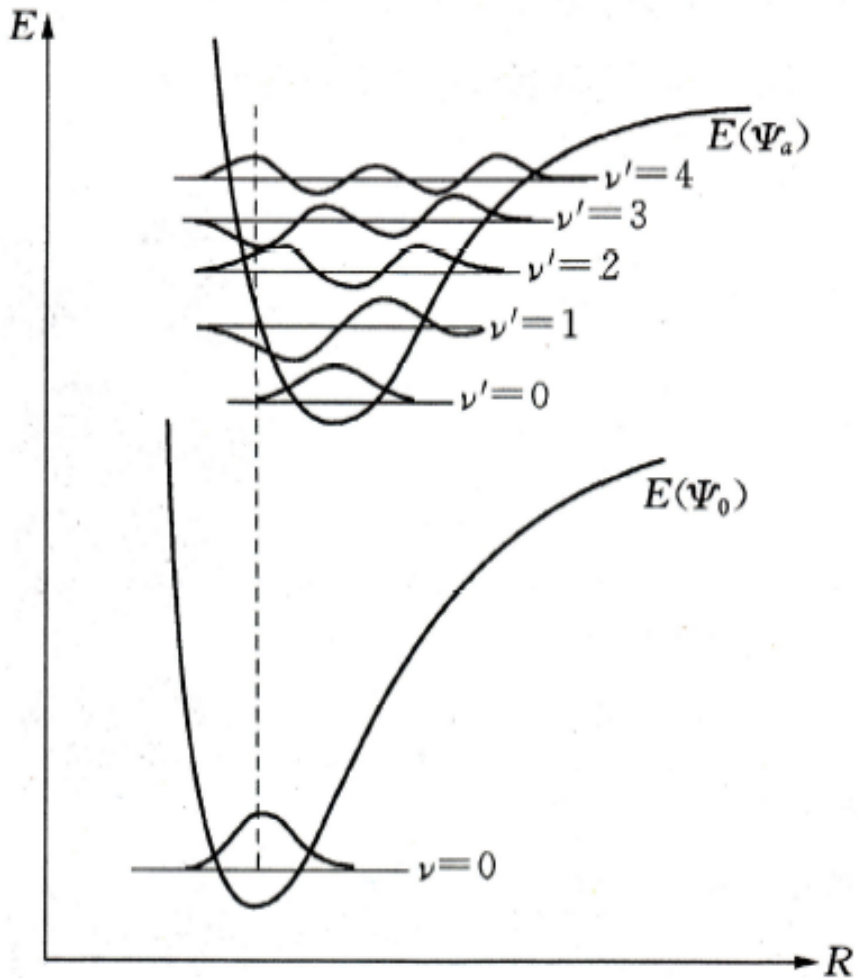


图 2.1.5 Franck-Condon 原理示意

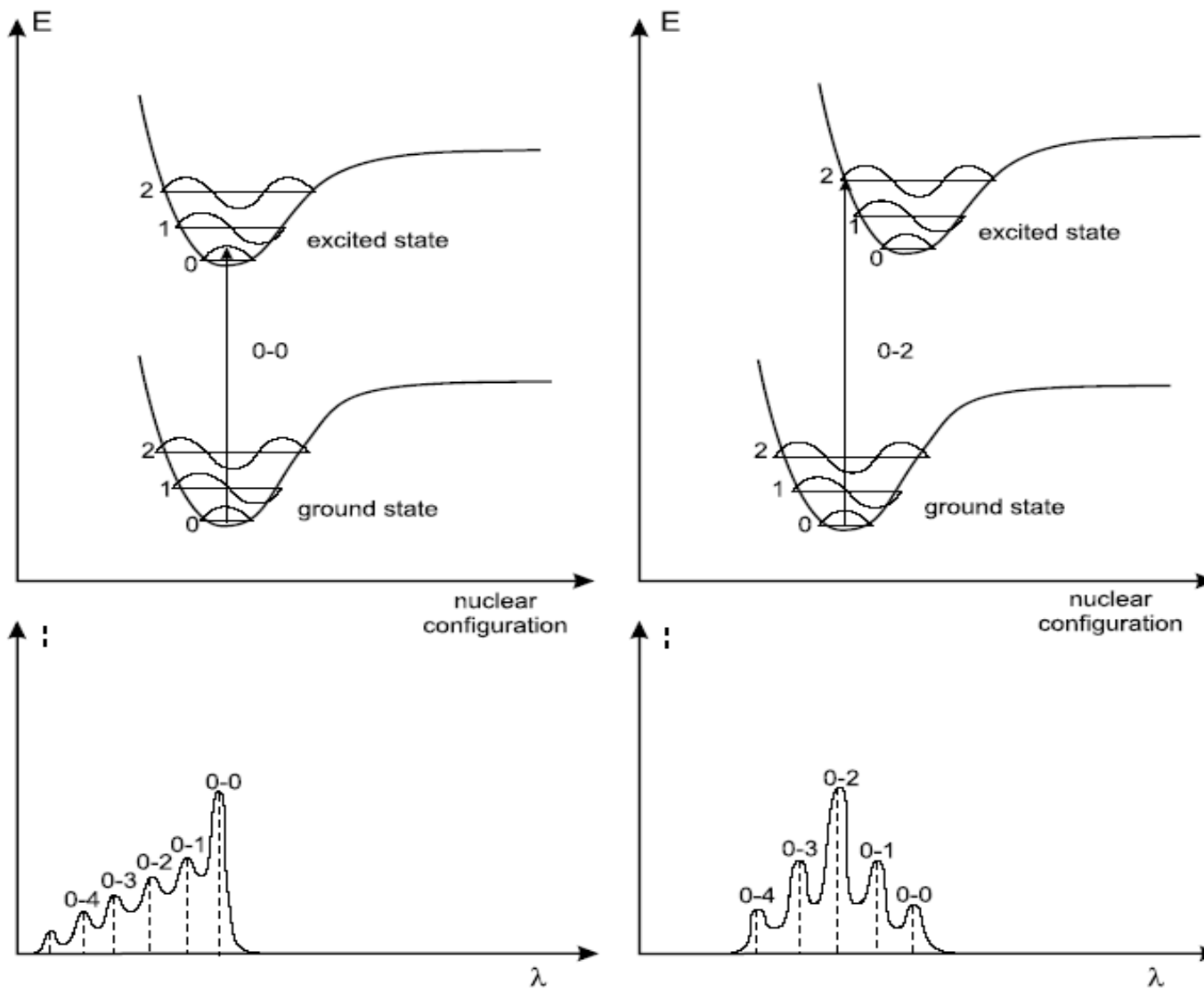


Fig. 2.4. Top: Potential energy diagrams with vertical transitions (Franck–Condon principle). Bottom: shape of the absorption bands; the vertical broken lines represent the absorption lines that are observed for a vapor, whereas broadening of the spectra is expected in solution (solid line).

FC原理的吸收光谱示意图

荧光发射过程及其中的物理

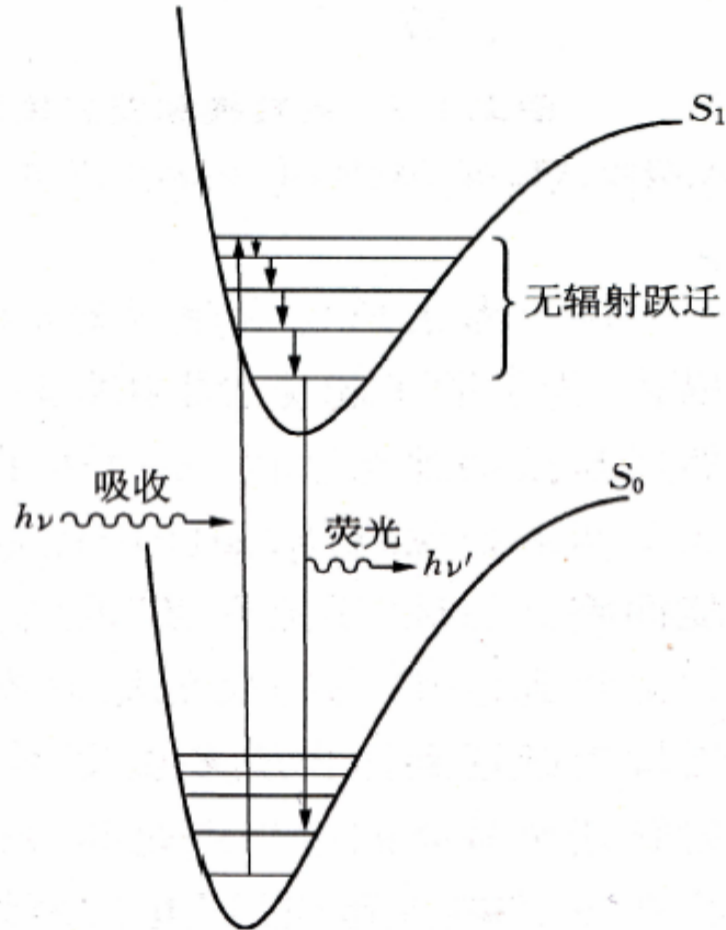


图 2.1.6 荧光发射过程示意^[6]

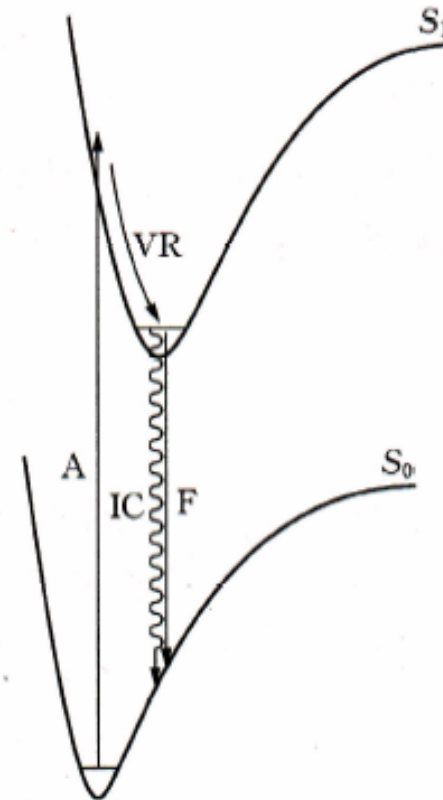


图 2.1.7 内转换和荧光辐射
(A,吸收; VR,振动驰豫; IC,内转换; F,荧光。)

内转换和荧光发射存在竞争关系

系间窜越 (ISC) 与磷光发射 (P)

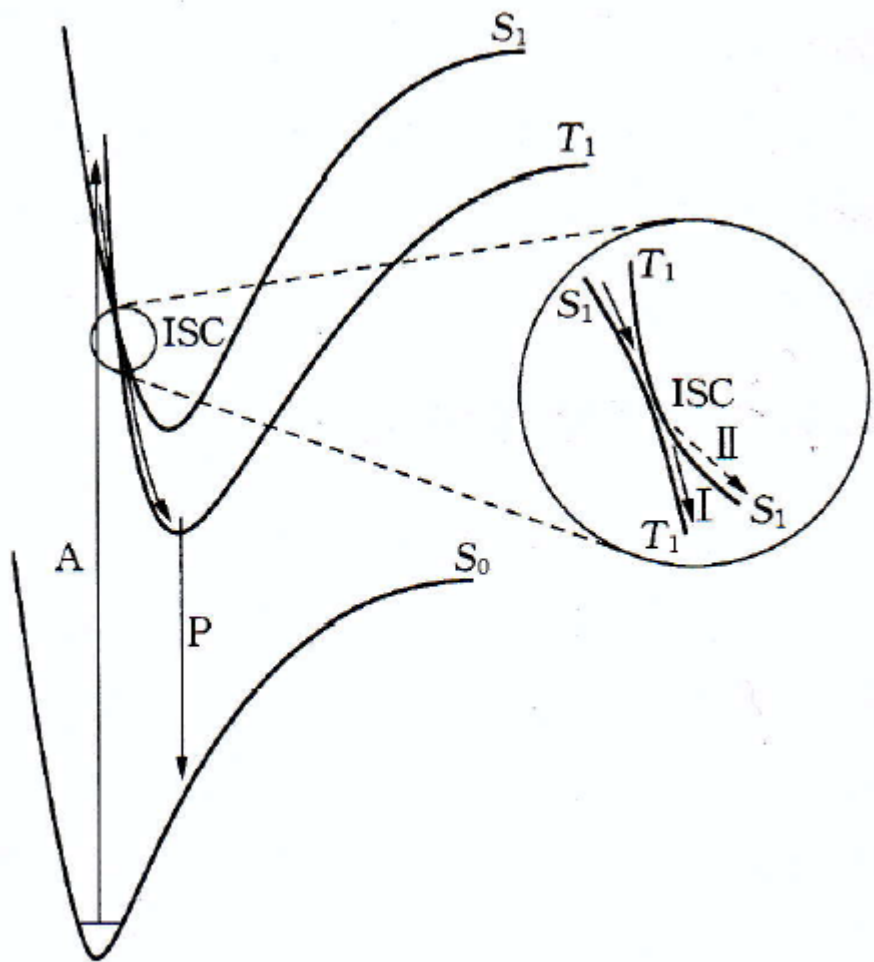


图 2.1.8 系间窜越(ISC)与磷光发射(P)

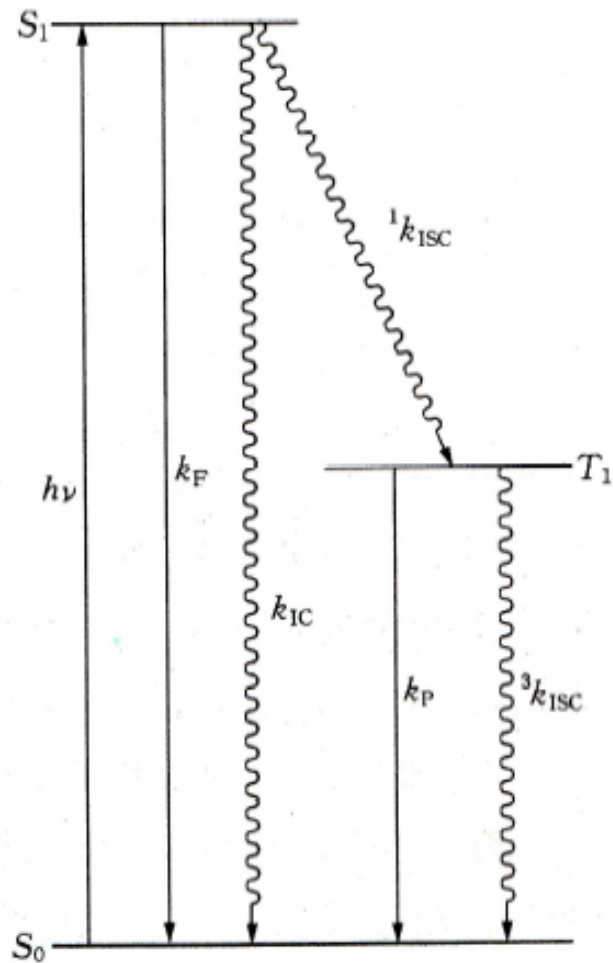
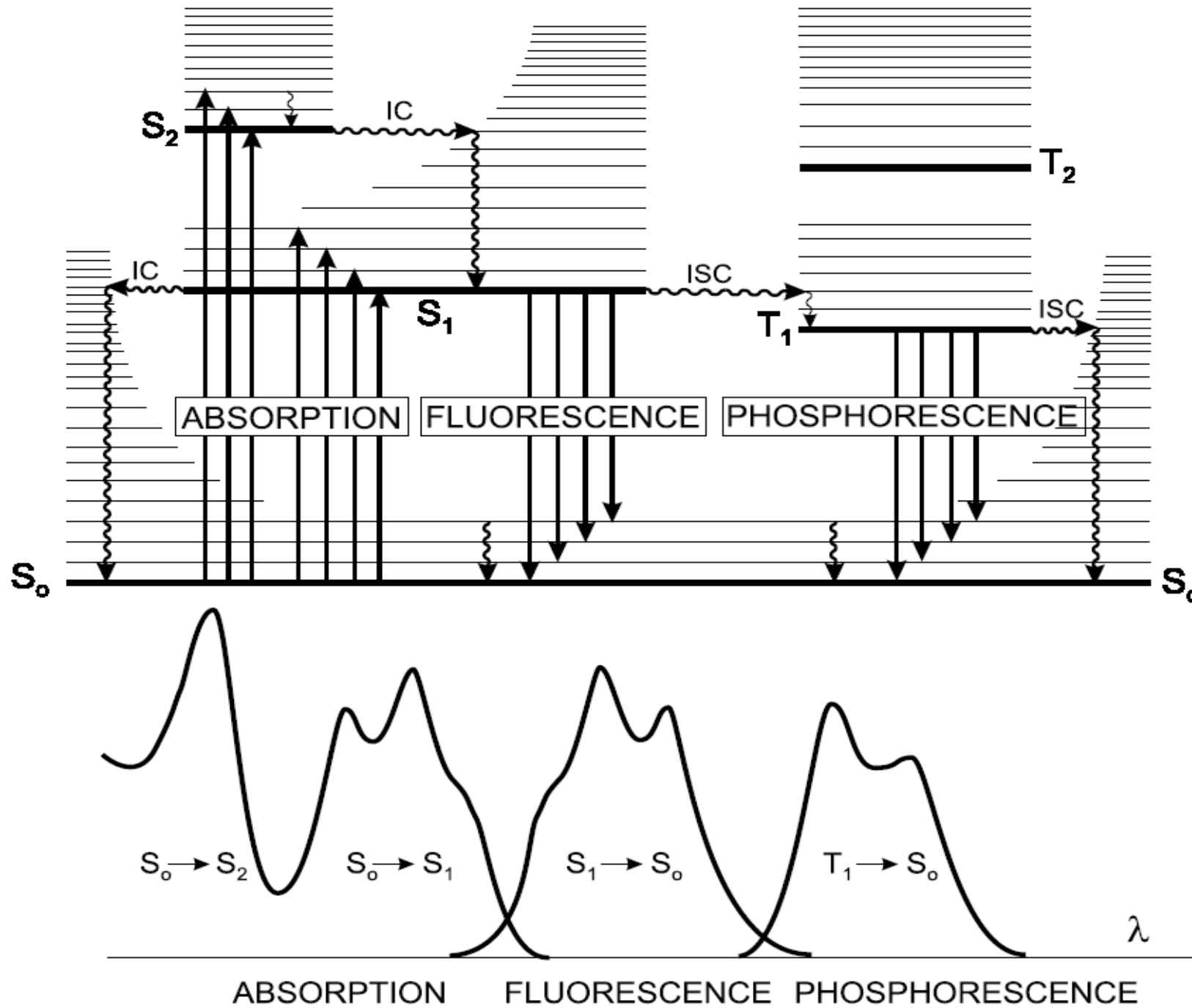


图 2.1.12 光物理过程的各个步骤及速率常数表示



上页的图就是著名的荧光和磷光的Jablonski图

可以看到：吸收谱和荧光谱是镜面对称的；由于振动弛豫（VR）的存在，荧光谱相对于吸收谱红移。

SPP可以参与过程：通过近场增益增大吸收、通过纳米结构改变电磁场的空间态（模式）密度（或荧光寿命），从而影响荧光和磷光发射。

下表中给出Jablonski图中各个物理过程的特征时间

CHARACTERISTIC TIMES	
absorption	10^{-15} s
vibrational relaxation	10^{-12} - 10^{-10} s
lifetime of the excited state S ₁	10^{-10} - 10^{-7} s → fluorescence
intersystem crossing	10^{-10} - 10^{-8} s
internal conversion	10^{-11} - 10^{-9} s
lifetime of the excited state T ₁	10^{-6} -1 s → phosphorescence

荧光和磷光的量子产率 (quantum yield)

k_r^S : rate constant for radiative deactivation $S_1 \rightarrow S_0$ with emission of fluorescence

k_{ic}^S : rate constant for internal conversion $S_1 \rightarrow S_0$.

k_{isc} : rate constant for intersystem crossing.

$$\text{激发态寿命 } \tau_S = \frac{1}{k_r^S + k_{nr}^S}$$

$$k_{nr}^S = k_{ic}^S + k_{isc}.$$

For deactivation from T_1 , we have

k_r^T : rate constant for radiative deactivation $T_1 \rightarrow S_0$ with emission of phosphorescence.

k_{nr}^T : rate constant for non-radiative deactivation (intersystem crossing) $T_1 \rightarrow S_0$.

荧光量子产率

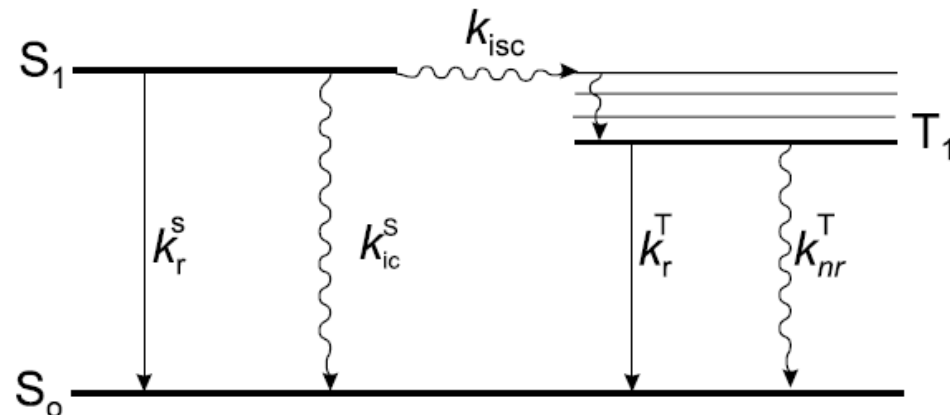
$$\Phi_F = \frac{k_r^S}{k_r^S + k_{nr}^S} = k_r^S \tau_S$$

系间窜越的比例

$$\Phi_{isc} = \frac{k_{isc}}{k_r^S + k_{nr}^S} = k_{isc} \tau_S$$

磷光量子产率

$$\Phi_P = \frac{k_r^T}{k_r^T + k_{nr}^T} \Phi_{isc}$$



$$k_{nr}^S = k_{ic}^S + k_{isc}$$

分子间能量转移过程 (donor and acceptor)

可分为辐射能量转移和非辐射能量转移

辐射能量转移：处于基态的受体吸收处于激发态的给体发出的一个光子而被激发，给体和受体间不直接接触，相互作用距离5到10纳米。

非辐射能量转移：没有发出光子的过程，有右边以下几种情况：

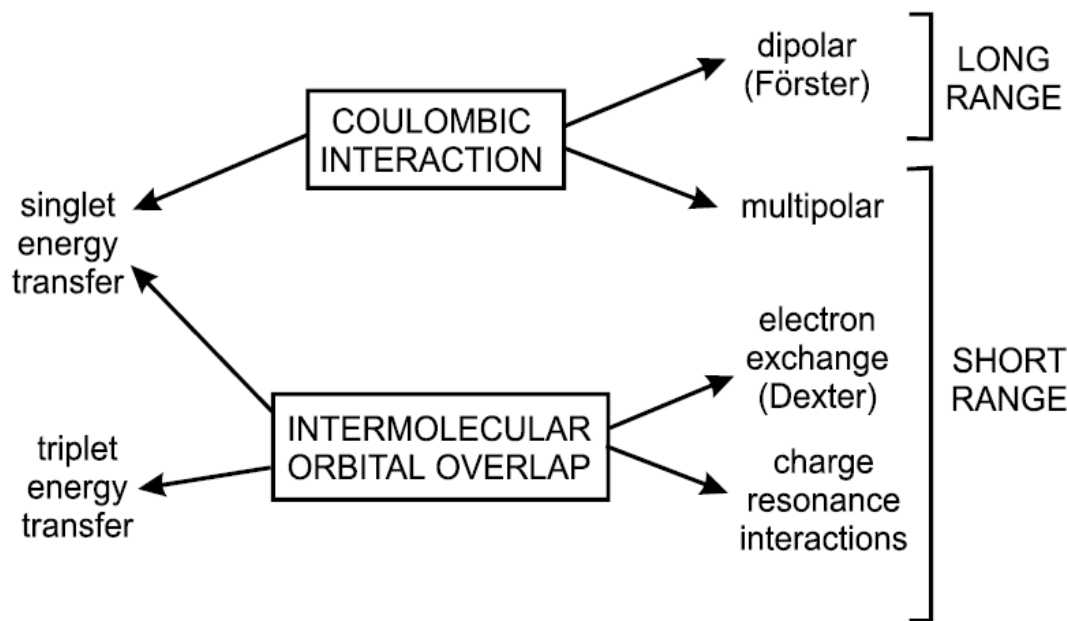
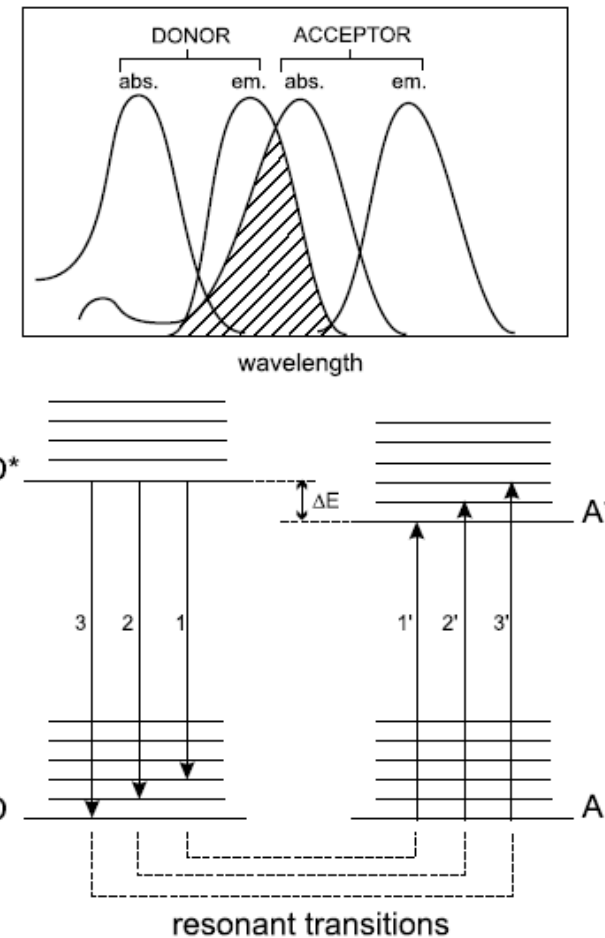
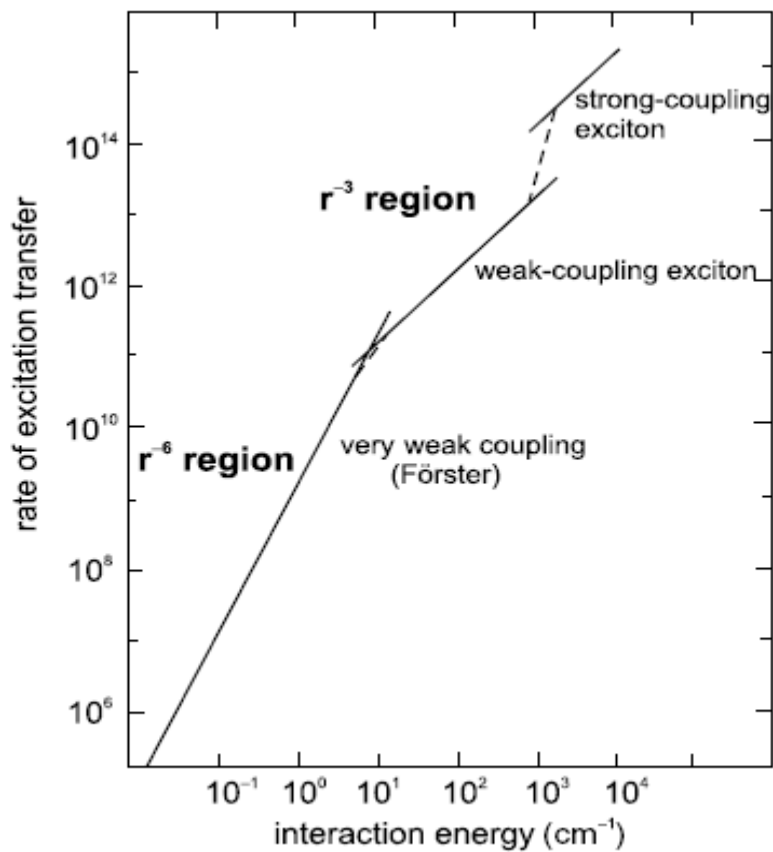


Fig. 4.13. Types of interactions involved in non-radiative transfer mechanisms.

Forster能量转移过程



Forster能量转移：外加电磁场使分子产生诱导偶极，通过偶极偶极间的长程相互作用实现能量转移，相互作用距离5到10纳米。
右图表示共振能量转移，Forster能量转移是其中一种。
左图表示各种不同结合能下能量转移率。

量子点简介

电子的物质波特性取决于其费米波长：

$$\lambda_F = 2\pi / k_F$$

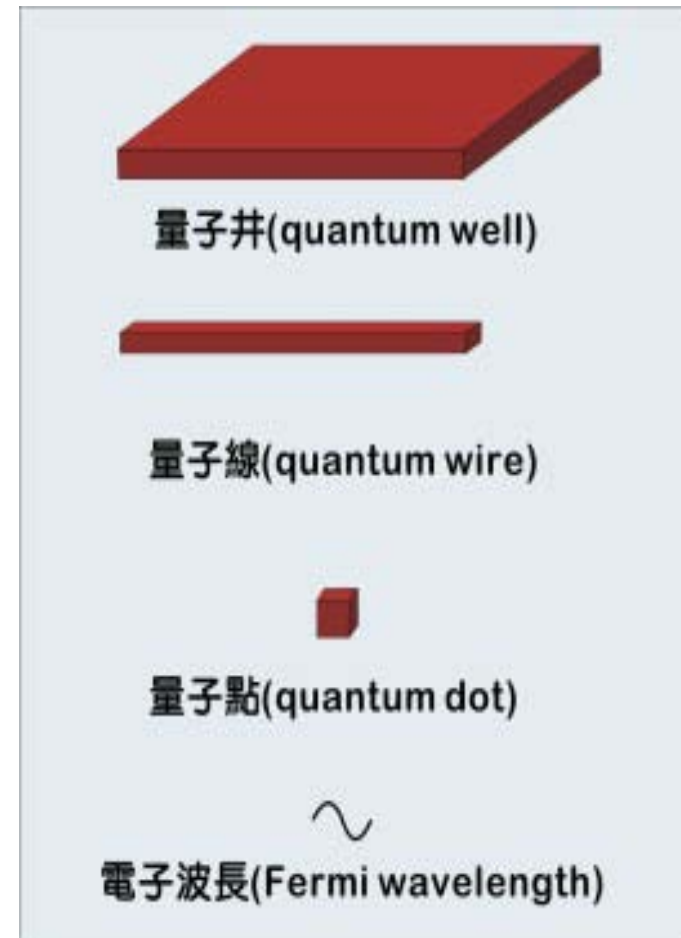
在一般的材料中，电子的波长远小于材料的尺寸，因此量子局限效应不显著。

量子阱：如果将某一个维度的尺寸缩到小于一个波长，此时电子只能在另外两个维度所构成的二维空间中自由运动；

量子线：如果我们再将另一个维度的尺寸缩到小于一个波长，则电子只能在一维方向上运动；

量子点：当三个维度的尺寸都缩到一个波长以下时，就成为量子点了。

由此可知，真正的关键尺寸是由电子在材料内的费米波长决定，一般在百纳米内。



(网上查到，出处不明)

致谢：
李佳、王珞珈和任攀

